bioRxiv preprint doi: https://doi.org/10.1101/2020.11.10.377481; this version posted August 18, 2021. The copyright holder for this preprint (which was not certified by peer review) is the author/funder, who has granted bioRxiv a license to display the preprint in perpetuity. It is made available under aCC-BY-NC-ND 4.0 International license.

Conflict over fertilization underlies the transient evolution of reinforcement

Catherine A. Rushworth[1,2], Alison M. Wardlaw[1], Jeffrey Ross-Ibarra[2,3] and Yaniv Brandvain[1,*]

[1]Dept. of Plant and Microbial Biology, University of Minnesota, St. Paul, MN, USA, [2]Dept. of Evolution and Ecology and Center for Population Biology, University of California, Davis, CA, USA, [3]Genome Center, University of California, Davis, CA, USA

ABSTRACT When two species meet in secondary contact, the production of low fitness hybrids may be prevented by the adaptive evolution of increased prezygotic isolation, a process known as reinforcement. Theoretical challenges to the evolution of reinforcement are generally cast as a coordination problem—e.g., recombination may break the association between trait and preference loci. However, the evolution of reinforcement also poses a potential conflict between mates. For example, the opportunity costs to hybridization may differ between the sexes or species. This is particularly likely for reinforcement based on postmating prezygotic (PMPZ) incompatibilities, as the ability to fertilize both conspecific and heterospecific eggs is beneficial to male gametes, but heterospecific mating may incur a cost for female gametes. We develop a population genetic model of interspecific conflict over reinforcement inspired by "gametophytic factors", which act as PMPZ barriers among *Zea mays* subspecies. We demonstrate that this conflict results in the transient evolution of reinforcement—after females adaptively evolve to reject gametes lacking a signal common in conspecific gametes, this gamete signal adaptively introgresses into the other population. Ultimately the male gamete signal fixes in both species, and prezygotic isolation returns to pre-reinforcement levels. We interpret geographic patterns of isolation among *Z. mays* subspecies in light of these findings, and suggest when and how this conflict can be resolved. Our results suggest that sexual conflict over fertilization may pose an understudied obstacle to the evolution of reinforcement via PMPZ incompatibilities.

KEYWORDS Reinforcement, Sexual conflict, Speciation, Postmating prezygotic

Introduction

In the highlands of Mexico, a wild teosinte, *Zea mays* ssp. *mexicana*, often grows alongside and hybridizes with its domesticated relative *Zea mays* ssp. *mays* (hereafter, maize) (Hufford *et al.* 2013). In these locations, maize-teosinte hybrids are often disfavored—hybrids are removed from maize fields by anthropogenic weeding and maize traits expressed in teosinte environments are likely maladaptive (Wilkes 1977), leading to genome wide selection against admixture with maize despite adaptive introgression of some loci (Calfee *et al.* 2021). When sympatric with maize, this teosinte subspecies tends to shows elevated pollen discrimination—three separate stylar-expressed loci underlie preferential fertilization by teosinte-like pollen (Moran Lauter *et al.* 2017; Lu *et al.* 2014, 2019; Wang *et al.* 2018; Lu *et al.* 2020). A straightforward explanation for this observation is that postmating prezygotic (hereafter PMPZ) isolation has evolved by reinforcement—that is, this barrier may represent an adaptive enhancement of reproductive isolation favored because it minimizes the misplaced reproductive effort spent in producing low-fitness hybrids (Dobzhansky 1937; Servedio and Noor 2003). However, this explanation is insufficient; despite effectively rejecting pollen from allopatric maize, these barriers appear ineffective with pollen from sympatric maize (Kermicle *et al.* 2006; Kermicle and Evans 2010), where selection for reinforcement should be strongest.

What could explain this pattern, in which a population in sympatry with another displays enhanced reproductive isolation that is only effective against allopatric populations of heterospecifics, and what are its implication for the process of speciation? In this case, this pattern is not attributable to the loss of isolation upon secondary contact, because allopatric teosinte do not reject maize pollen (Kermicle *et al.* 2006; Kermicle and Evans 2010). Nor can this case be explained by complex speciation, in which teosinte sympatric with maize are more recently diverged from maize than are allopatric teosinte, as this is incompatible with both genetic evidence and the history of maize domestication (Ross-Ibarra *et al.* 2009). Rather, we consider the possibility that this pattern—a biogeographic distribution that runs counter to the pattern of enhanced incompatibility in sympatry expected under reinforcement, but which nonetheless displays a novel prezygotic barrier when populations exchanging genes produce maladapted hybrids—is a footprint of the historical evolution and collapse of reinforcement driven by a conflict between the sexes over fertilization. This possibility has broad implications beyond the motivating case of *Z. mays* subspecies, as it makes clear that a conflict between the sexes over mating presents a largely overlooked (but see Parker and Partridge 1998, for earlier ideas along these lines) challenge to the evolution of reinforcement.

Reinforcement is generally conceptualized as the evolution

* Dept. of Plant and Microbial Biology, University of Minnesota, St. Paul, MN, USA
E-mail: ybrandva@umn.edu

bioRxiv preprint doi: https://doi.org/10.1101/2020.11.10.377481; this version posted August 18, 2021. The copyright holder for this preprint (which was not certified by peer review) is the author/funder, who has granted bioRxiv a license to display the preprint in perpetuity. It is made available under aCC-BY-NC-ND 4.0 International license.

of enhanced prezygotic isolation (e.g. Felsenstein 1981) via female preference or trait matching (Kopp *et al.* 2018). These mechanisms implicitly assume either that males and females have a shared interest in avoiding the production of maladapted hybrids, or that preventing the production of low-fitness hybrid offspring is beneficial to females and an opportunity cost to males—that is, any fitness benefit to females of attracting a heterospecific mate would be small, relative to the loss of conspecific mating opportunities for males. However, reproductive interactions are often more fractious than this—the costs of reproductive effort can differ by sex and/or reproductive stage (Arnqvist and Rowe 2005). For example, in some cases the benefit of siring low fitness hybrids may exceed the opportunity cost for a male but not for a female (in other words, present an overall benefit to only males). In such cases, male and female interests are not always aligned, and sexual conflict over the hybridization rate (Parker and Partridge 1998) may create an often overlooked hurdle to the evolution of reinforcement.

Inspired by PMPZ incompatibilities between *Z. mays* subspecies, we develop a population genetic model to evaluate how this sexual conflict over hybridization can alter the evolution of reinforcement. Specifically, we model PMPZ incompatibilities as "gametophytic factors", consisting of a stylar locus for which individuals with an incompatible allele can only be fertilized by pollen bearing the allele that can overcome this incompatibility. From the female perspective, there are multiple chances to get conspecific pollen, so stylar alleles that discriminate against interspecific pollen in favor of compatible conspecific pollen will be favored; and from the male perspective, pollen grains on heterospecific styles cannot be redirected, so universally compatible pollen alleles will be favored. We show that asymmetry in costs and benefits of hybridization faced by males and females results in the transient evolution of reinforcement, as, following the initial adaptive evolution of the stylar barrier, alleles that confer male compatibility adaptively introgress across populations. This model thus generates a signature consistent with observations in *Z. mays* subspecies. Notably, we find a similar outcome when two populations have their own unique incompatibilities, suggesting that this result is attributable to asymmetric costs and benefits experienced by the sexes, and not asymmetry in cross success.

Beyond this motivating case, our model suggests that sexual conflict—a mismatch between optimal fertilization outcomes of each sex—makes novel predictions and provides potential explanations for numerous patterns in nature. Our results are particularly relevant to many potential cases of reinforcement by gamete recognition in plants, broadcast spawners (e.g. Lysin/VERL in abalone (Swanson and Vacquier 1998) or Bindin/EBR1 (Metz *et al.* 1994) in sea urchins), and even cases of internal fertilization in which premating isolation is inefficient, costly, or otherwise unpreferred (Turissini *et al.* 2017). In these situations, we predict that reinforcement by PMPZ will be rare, transient, or involve a trade-off between heterospecific and conspecific fertilization.

Results

Model overview

We deterministically iterate a model inspired by empirical observations in a wild teosinte subspecies of *Zea mays*, where pairs of tightly-linked loci—termed gametophytic factors—mediate PMPZ (in)compatibility with domesticated maize (Moran Lauter *et al.* 2017; Lu *et al.* 2014, 2019; Wang *et al.* 2018). We therefore refer to maize and teosinte in our model to simplify biological interpretation. We note that our use of the terms "male" and "female" refer to male and female function, or pollen and pistil function, respectively. A full description of this iteration is in Supp. Text S1, and the code is available at https://github.com/carushworth/gameto-theory.

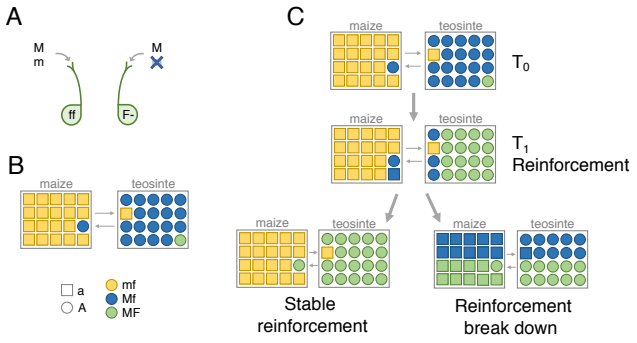

Figure 1 Model dynamics (A) Gametophytic factors of maize and teosinte. The dominant *F* allele encodes a stylar fertilization barrier that can only be overcome by the pollen-expressed compatibility allele *M*. **(B)** Pollen flows between two diverged populations (hereafter maize and teosinte) facing different selective pressures. Colors denote gametophytic factor haplotypes, and shapes signify genotypes at a divergently selected allele. Initially, maize is fixed for the non-barrier *f* allele and the incompatible pollen-expressed *m* allele, and a locally adaptive allele at adaptation locus $\mathcal{A}$ (haplotype *mfa*). Teosinte is initially fixed for the pollen compatibility allele and its locally adapted allele, with a rare stylar barrier allele (haplotypes *MfA* and *MFA*). **(C)** We run the model from this initial parameterization at generation T_0 until the *F* allele reaches its equilibrium frequency, shown in the bottom panel. If some reinforcement evolves by time T_1 (equivalent to the *F* allele increasing in frequency in teosinte), two further outcomes are possible: the *M* allele may introgress onto the locally adaptive background and fix in both populations, leading to the breakdown of reinforcement; or, in extreme cases, the *M* allele may fail to spread in maize while *F* continues to spread through the teosinte population, leading to complete reinforcement.

Population structure, migration, and pollination: We model two demes—one representing a "maize" and the other a "teosinte" environment (i.e. a two-island model) with all migration occurring via pollen. Every generation, a proportion $g_{\text{maize}\to\text{teo}}$ of pollen in the teosinte environment originates from plants in the maize environment, and $g_{\text{teo}\to\text{maize}}$ pollen in the maize environment originates in the teosinte environment (Figure 1B). Within each environment, pollen lands on styles at random.

Fertilization: Although pollination within a deme is random, fertilization is controlled by a two-locus PMPZ incompatibility (*sensu* Lorch and Servedio 2007). The stylar-acting locus $\mathcal{F}$ is under diploid control. We assume the incompatibility is dominant—i.e. styles with one or two *F* alleles discriminate between pollen genotypes, preferentially accepting pollen with the *M* allele (Figure 1A). Fertilization is random in styles homozygous for the compatibility allele *f*. This notation differs from that in the existing literature, which treats gametophytic factors as four haplotypes rather than pairs of two locus genotypes (see

bioRxiv preprint doi: https://doi.org/10.1101/2020.11.10.377481; this version posted August 18, 2021. The copyright holder for this preprint (which was not certified by peer review) is the author/funder, who has granted bioRxiv a license to display the preprint in perpetuity. It is made available under aCC-BY-NC-ND 4.0 International license.

Supp. Text S2).

We assume no direct fitness cost to the female incompatibility (e.g. there is no preference cost) or male compatibility. We further assume that the stylar barrier F is initially rare in teosinte (1% frequency) and absent in maize, and that the male compatibility allele M is fixed in teosinte and absent in maize. Variation in the initial frequency of M in teosinte, however, has nearly no effect on the outcome (Fig. S1). Finally, we assume that styles with barrier genotypes cannot be fertilized by incompatible pollen; relaxing this assumption results in expected quantitative differences in results, but does not change our qualitative conclusions (Fig. S2).

Selection: We model isolation by local adaptation (following Kirkpatrick 2001) with extrinsic isolation driven by n local adaptation loci, each noted as $\mathcal{A}_i$, where the subscript i is an arbitrary index of loci. Selection coefficients are s_{maize} and s_{teo} in maize and teosinte environments, respectively, and fitness w is multiplicative within and among loci, $w = (1-s)^{\#\text{ maladapted alleles}}$.

Recombination and genome structure: We initially assume a locus order of $\mathcal{A}_1\mathcal{M}\mathcal{F}$, with recombination rates $r_{\mathcal{A}_1\mathcal{M}}$ and $r_{\mathcal{M}\mathcal{F}}$, and that local adaptation loci $\mathcal{A}_2$ through $\mathcal{A}_n$ are unlinked to one another and the $\mathcal{M}$ and $\mathcal{F}$ loci. After presenting these results, we explore alternative marker orders.

A second gametophytic factor: To ensure that our results are not due to asymmetry of variation for female choice in only one population, we introduce a second unlinked incompatibility locus: $\mathcal{A}_z\mathcal{M}_z\mathcal{F}_z$. This second barrier acts like the first, detailed above, but F_z is initially rare in maize and absent in teosinte, and M_z is initially fixed in maize and absent in teosinte.

Sexual Conflict Leads to Transient Reinforcement

When reinforcement evolves, it is almost always transient. The rise and fall of reinforcement, as well as allele and haplotype frequency dynamics across generations for one set of parameter values, is shown in Figure 2 (see figure legend for parameter values).

In this example, substantial reinforcement evolves and can near completion (Phase 1, Fig. 2A), but is ultimately fleeting. Reinforcement begins as the female incompatibility allele F increases in frequency in teosinte (Fig. 2B), and prevents fertilization by locally maladapted immigrant maize haplotypes. This maintains both the high frequency of locally adapted (A) and pollen compatible (M) alleles in teosinte (Fig. 2C) and the near complete linkage disequilibrium between them (note the large value of r^2_{AM} in Fig. 2D,F). Because F is rare in maize during this early phase, the direct advantage to the M allele in maize is initially very small. The allele remains at low frequency for some time, as it is removed by linked viability selection (see discussion of Fig. 3, below).

Subsequently, however, the male compatibility allele M recombines onto the a background, undermining reinforcement as it spreads and introgresses into maize (Phase 2 of Fig. 2). That is, migration of teosinte haplotypes into maize enables recombination of M onto the locally adapted maize background. As the aMf haplotype sweeps through maize (Fig. 2E), LD between locally adapted and pollen compatibility alleles, r^2_{AM} decreases in both populations (Fig. 2D,F).

This decrease in LD between pollen expressed and locally adaptive alleles attenuates selection against the stylar incompatibility allele F in maize, allowing the modest mating advantage to facilitate the spread of the M allele (Fig. 2B). As M rises in

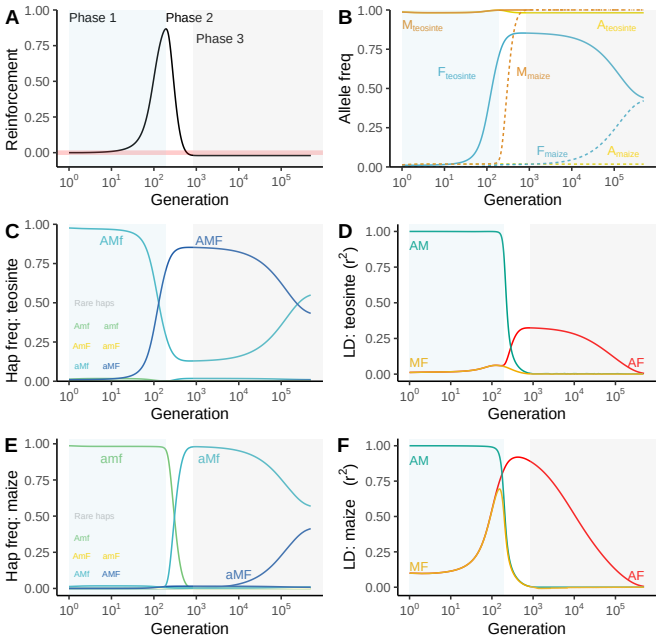

Figure 2 The rise and fall of reinforcement in three phases. A stylar barrier allele F preventing fertilization by m pollen spreads in teosinte (Phase 1: light blue). The compatible pollen allele, M, next introgresses into the maize population and spreads (Phase 2: white). After M fixes, the barrier F slowly disassociates from the teosinte background, eventually equilibrating in both populations (Phase 3: light grey). (**A**) Reinforcement is transient, building in Phase 1 and breaking down in Phase 2. The pink line shows zero reinforcement. (**B**) Allele frequencies in both populations, with solid lines in teosinte and dashed lines in maize. The F allele increases in teosinte, followed by fixation of M and subsequent neutrality of F. (**C**) Haplotype frequencies over time in teosinte. (**D**) Gametic linkage disequilibrium (LD), measured as r^2, for all pairs of loci in teosinte. (**E**) Haplotype frequencies over time in maize. (**F**) Gametic LD in maize for all pairs of loci. All measures describe populations after selection and before recombination. This figure illustrates a single set of parameter values with one adaptive locus. Selection: $s_{\text{teo}} = s_{\text{maize}} = 0.75$; Migration: $g_{\text{maize}\to\text{teo}} = g_{\text{teo}\to\text{maize}} = 0.1$; Recombination: $r_{\mathcal{AM}} = r_{\mathcal{MF}} = 0.0001$; Allele frequencies: $f_{M0,\text{teo}} = 1$, $f_{M0,\text{maize}} = 0$, $f_{F0,\text{teo}} = 0.01$, $f_{F0,\text{maize}} = 0$.

frequency and eventually fixes across the metapopulation (Fig. 2B), migrant pollen are no longer rejected, indicated by reinforcement approaching zero in Fig. 2B. At this point, selection against F in maize weakens until it is completely neutral (see discussion of Fig. 3, below). From then on, F slowly equilibrates across populations (Phase 3 of Fig. 2A) as continued migration and recombination between the $\mathcal{A}$ and $\mathcal{F}$ loci decreases LD between them (Fig. 2D,F).

Allele frequency change across the life cycle

We now show how migration, fertilization and selection drive changes in allele frequencies across the life cycle (Fig. 3). See Supp. Text S3 for exact expressions.

Migration homogenizes allele frequencies. The change in allele frequency by pollen migration is the difference in allele frequen-

bioRxiv preprint doi: https://doi.org/10.1101/2020.11.10.377481; this version posted August 18, 2021. The copyright holder for this preprint (which was not certified by peer review) is the author/funder, who has granted bioRxiv a license to display the preprint in perpetuity. It is made available under aCC-BY-NC-ND 4.0 International license.

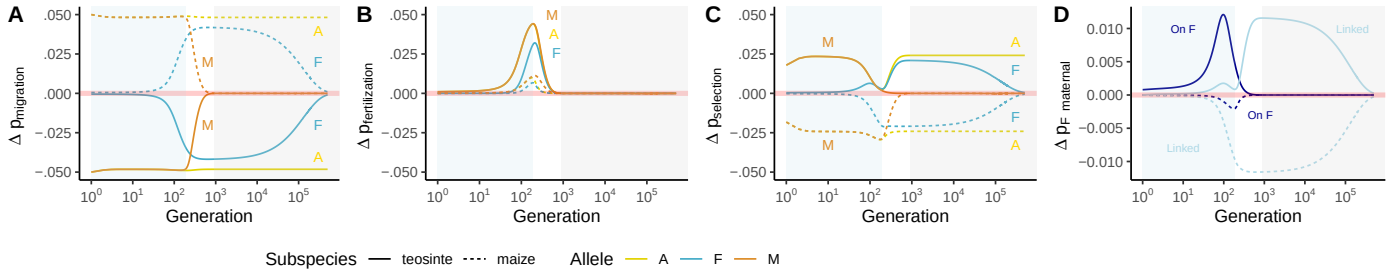

Figure 3 Allele frequency change across the life cycle. Alleles A, M, and F, which are located in teosinte, change in frequency across the metapopulation as described in the main text. The transparent thick pink line at zero denotes no change in allele frequency during this life phase. During migration (**A**), teosinte alleles decrease in frequency in teosinte (solid line, indicated by values below the zero line) and increase in maize (dotted line, indicated by values above the zero line). During fertilization (**B**), teosinte alleles increase in both populations. This effect is strongest in their local population, due to a direct fertilization advantage of M in combination with linkage disequilibrium among loci. (**C**) Selection on A in teosinte increases its frequency throughout, while the frequency of A in maize is consistently negatively impacted. Linkage between A and M results in overlapping lines during phase 1. The transition from phase 1 to phase 2 is marked by a dip in the frequency of A, caused by near-fixation of F on the A background, as migrant maize haplotypes are unable to penetrate the teosinte population at the peak of F's frequency. (**D**) decomposes selection on F into two components of allele frequency change. In dark blue we show "reinforcing selection" (the F allele frequency change attributable to preferential fusion with M), which enables avoidance of the maladapted a allele in teosinte. In light blue we show the allele frequency change attributable to the incidental gametic phase linkage between F and A; see Methods for more detail. **Parameter values:** Figures generated with one locally adaptive allele with $s_{\text{teo}} = s_{\text{maize}} = 0.75$, migration rates, $g_{\text{maize}\to\text{teo}} = g_{\text{teo}\to\text{maize}} = 0.1$, and recombination rates $r_{\mathcal{AM}} = r_{\mathcal{MF}} = 0.0001$. Initially, populations are locally adapted ($f_{\mathcal{A},\text{teo}} = 1 - f_{\mathcal{A},\text{maize}} = 1$), with M fixed in teosinte and absent in maize, and F at frequency 0.01 in teosinte and absent in maize. Background shading marks phase one (light blue), phase two (white), and phase three (grey) of transient reinforcement, as in Figure 2.

cies between populations weighted by the migration rate (Eq. S1). This homogenizes allele frequencies (Figure 3A), which can be seen as the decrease in frequency of all teosinte alleles in teosinte (solid lines for A, M, and F are all always less than zero) and the increase in frequency of all teosinte alleles in maize (dashed lines are always greater than zero).

The stylar barrier F favors the male compatibility allele M and indirectly favors alleles in LD with M: Assuming dominance of the female postmating incompatibility allele, the fertilization advantage of M depends on the proportion of incompatible styles in the present generation (i.e. those that are heterozygous or homozygous for F). This equals $1 - p_{ff}$, where p_{ff}, the frequency of styles homozygous for the f allele, differs from p_f^2 due to non-random fertilization. As we derive in Eqs. S2 and S3, the increase in frequency of allele M from pollen to paternally-derived haplotypes equals

$$\Delta p_{\text{ fertilization}} = (1 - p_{ff}) \frac{p'_M p'_m c}{1 - c p'_m} \tag{1}$$

where c is the intensity of discrimination against incompatible pollen-expressed alleles, and the super-script $'$ indicates that allele frequencies in pollen are taken after migration, while female frequencies are not noted by $'$ because only pollen migrate.

In line with this analytical result, Figure 3B shows that the frequency of the M allele in both populations always increases during fertilization until it fixes at the start of Phase 3. In addition to directly increasing the frequency of the M allele, selection indirectly favors alleles in LD with it (Eq. S4-S5). Because LD among all teosinte alleles is > 0, both the A and F alleles increase in frequency through a fertilization advantage to M in both populations (Fig. 3B). This incompatibility system generates a *trans* association between maternally-derived $\mathcal{F}$ and paternally-derived $\mathcal{M}$ alleles (Eq. S6).

Allele frequency change by natural selection follows standard expectations: Selection increases the frequency of the locally adapted allele at locus $\mathcal{A}$ in each environment (Fig. 3C, Eq. S7-S8). Likewise, linked selection on M and F alleles (Fig. 3C) reflect LD with the locally adapted alleles (Fig. 2D and F), with alleles in positive LD with A increasing in frequency in teosinte and decreasing in frequency in maize (Eq. S9).

Selection favors the female incompatibility in teosinte and disfavors it in maize: In the Methods, we describe our novel approach to partition the extent to which the increase in frequency of the female isolating barrier F is attributable to reinforcing selection (Hopkins *et al.* 2014) versus linked selection. The initial increase in frequency of F in teosinte (during Phase 1) is largely attributable to selection for reinforcement, but its persistence advantage, once M has reached appreciable frequency in maize, is attributable to linked selection (Fig. 3D). Both selection against this incompatibility (i.e. because it is preferentially fertilized by A bearing pollen) and linked selection (i.e. because it is in gametic phase LD with the locally maladapted A allele) acting on the $\mathcal{A}$ locus act to disfavor F in maize. Selection against the incompatibility in maize due to its effects on non-random fertilization weaken as recombination erodes LD between M and A, while indirect selection against F in maize weakens as recombination erodes LD between F and A (Fig. 3D).

Determinants of the strength and duration of reinforcement

We now show how varying parameter values influence the maximum amount (Fig. 4A-D) and duration (Fig. 4E-H) of reinforcement in the face of this conflict.

Reinforcement often requires strong selection: As the intensity of selection on the locally adaptive allele intensifies, the maximum extent (Fig. 4A) and total duration (Fig. 4E) of reinforcement both increase. With symmetric selection and symmetric

bioRxiv preprint doi: https://doi.org/10.1101/2020.11.10.377481; this version posted August 18, 2021. The copyright holder for this preprint (which was not certified by peer review) is the author/funder, who has granted bioRxiv a license to display the preprint in perpetuity. It is made available under aCC-BY-NC-ND 4.0 International license.

migration, selection on the local adaptation locus must be exceptionally strong for any reinforcement to evolve—e.g. even with $s = 0.3$ only very subtle reinforcement evolves for a very short time. However, other parameter choices—e.g. asymmetric migration or selection—can mediate the strength of selection required for reinforcement to evolve (see below).

With symmetric migration and asymmetric selection, the strength of selection in maize (i.e. the population without the stylar incompatibility) generally has a greater effect on the extent and duration of reinforcement than does the strength of selection in teosinte (Fig. 4B and F, respectively, and across migration rates in Fig. S3). This is because strong selection in maize minimizes the opportunity for M to recombine onto the locally adapted a background before the migrant MA haplotype is removed by selection.

The extent and symmetry of migration mediates reinforcement: With symmetric migration, intermediate migration rates always maximize the extent of reinforcement (Fig. 4A), while the duration of reinforcement decreases as the migration rate increases (Fig. 4E), regardless of the selection coefficient s.

The effect of asymmetric migration on the extent of reinforcement highlights the role of migration in mediating this conflict. Migration from maize to teosinte increases selection for reinforcement by increasing the number of maladapted immigrants, resulting in stronger reinforcement as $g_{\text{maize}\to\text{teo}}$ increases (Fig. 4C). By contrast, increasing migration from teosinte to maize accelerates the introgression of the M allele into maize, especially at higher migration rates, rapidly undermining reinforcement (Fig. 4G). With unidirectional migration from maize to teosinte, substantial reinforcement can persist for prolonged time periods (Fig. 4C,G).

Tight linkage between the male (in)compatibility locus $\mathcal{M}$ and a single local adaptation locus $\mathcal{A}$ results in greater reinforcement: When $\mathcal{A}$ and $\mathcal{M}$ are tightly linked, substantial reinforcement can evolve and last for some time. However, the strength and duration of reinforcement drops, initially modestly, and then quite precipitously, as the recombination rate increases, with nearly no reinforcement evolving when $\mathcal{A}$ and $\mathcal{M}$ are unlinked (Fig. 4D, H). The selection coefficient modulates this effect of recombination (Fig. S4): when selection is very strong (e.g. s > 0.6) some reinforcement can evolve, even when $\mathcal{A}$ and $\mathcal{M}$ are separated by up to a centiMorgan (i.e. $r_{AM} = 0.01$).

This result suggests that the rate of recombination between the local adaptation and male compatibility loci, $r_{\mathcal{AM}}$, underlies the sexual conflict over reinforcement. When $r_{\mathcal{AM}}$ is high, meaning $\mathcal{A}$ and $\mathcal{M}$ are loosely linked, M can more easily recombine onto the locally adapted a background, which facilitates its introgression. By escaping from the A background, M has greater long-term viability in maize than it would if it remained associated with the a allele, and thus the male benefit to overcoming the female barrier F is increased.

Linkage between female barrier and male (in)compatibility alleles does not strongly impact the amount or duration of reinforcement: Contrary to classic results of reinforcement theory (Felsenstein 1981), linkage between the male and female (in)compatibility alleles, $r_{\mathcal{MF}}$, has a very modest effect on the evolution of reinforcement. This effect is robust across most selection coefficients and most values of $r_{\mathcal{AM}}$ (Fig. 4D,H, reproduced in Fig. S5A,D). This result is not driven by marker order, as the extent and duration of reinforcement is largely insensitive to $r_{\mathcal{MF}}$ in models with loci in $\mathcal{MFA}$ order (Fig. S5B,E).

Instead, linkage between the local adaptation locus $\mathcal{A}$ and either $\mathcal{M}$ or $\mathcal{F}$ loci are critical to the evolution of reinforcement. Marker order $\mathcal{MAF}$ highlights the impact of recombination between the components of the PMPZ incompatibility complex on both the duration and intensity of reinforcement (Fig. S5C,F). We find that while both $r_{\mathcal{AM}}$ and $r_{\mathcal{FA}}$ modulate the level of reinforcement (Fig. S5C), the duration of reinforcement is nearly completely determined by recombination between the male compatibility $\mathcal{M}$ and local adaptation locus $\mathcal{A}$, $r_{\mathcal{AM}}$. Reinforcement duration is nearly independent of $r_{\mathcal{FA}}$ (Fig. S5E), consistent with sexual conflict undermining the evolution of reinforcement by PMPZ incompatibilities.

The presence of multiple unlinked local adaptation loci allows for (transient) reinforcement: Our results so far suggest that transient reinforcement by PMPZ incompatibilities requires tight linkage between divergently selected loci and loci underlying this incompatibility. However, the genetic architecture of local adaptation is often polygenic (Barghi *et al.* 2020), and this is also likely the case in diverged *Z. mays* subspecies (Wallace *et al.* 2014). Thus tight linkage between locally adaptive alleles and PMPZ incompatibilities may be biologically unrealistic.

We therefore investigate if weaker selection at more unlinked loci can allow reinforcement to transiently evolve by setting $r_{\mathcal{A}_1\mathcal{M}}$ to 0.5, and introducing up to four additional unlinked local adaptation $\mathcal{A}$ loci. Figure 5 shows that reinforcement can evolve when alternate alleles at numerous unlinked loci experience divergent selection in the two populations. This reflects recent work showing that, when numerous loci underlie reproductive isolation, selection on early-generation hybrids acts not against isolated loci, but on phenotypes underlain by pedigree relationships (Veller *et al.* 2019). While the selection coefficients displayed are still quite large, this suggests that weaker selection at many loci could likely result in the transient evolution of reinforcement.

An opposing gametophytic factor does not stabilize reinforcement: Finally, the transient nature of reinforcement by PMPZ incompatibilities could plausibly be due to asymmetry in female choice. That is, variation in female choice present in one population, but not the other, may underlie asymmetry that results in transience. To explore this possibility, we added an unlinked gametophytic factor and local adaptation locus to the maize population. While this complementary incompatibility allows reinforcement to begin at lower selection intensities and slightly expands the parameter space for which reinforcement stably evolves (Fig. S6A), reinforcement remains transient across most of the parameter space (Fig. S6B).

Discussion

For decades, researchers have presented theoretical and empirical challenges to the process of reinforcement, starting with Felsenstein's foundational paper (Felsenstein 1981), which identified recombination as a critical challenge to reinforcement. Since then, a large body of theory has investigated the circumstances that permit reinforcement to evolve, along with those that hinder it (reviewed in Kirkpatrick and Ravigné 2002). Despite its potential role in hampering speciation (Parker and Partridge 1998), sexual conflict over hybridization has received little attention in the literature, usually as a brief aside in papers concerning the role of sexual conflict in speciation more broadly (Parker and Partridge 1998; Gavrilets and Hayashi 2005; Gavrilets 2014). We identify the transient dynamics generated by

bioRxiv preprint doi: https://doi.org/10.1101/2020.11.10.377481; this version posted August 18, 2021. The copyright holder for this preprint (which was not certified by peer review) is the author/funder, who has granted bioRxiv a license to display the preprint in perpetuity. It is made available under aCC-BY-NC-ND 4.0 International license.

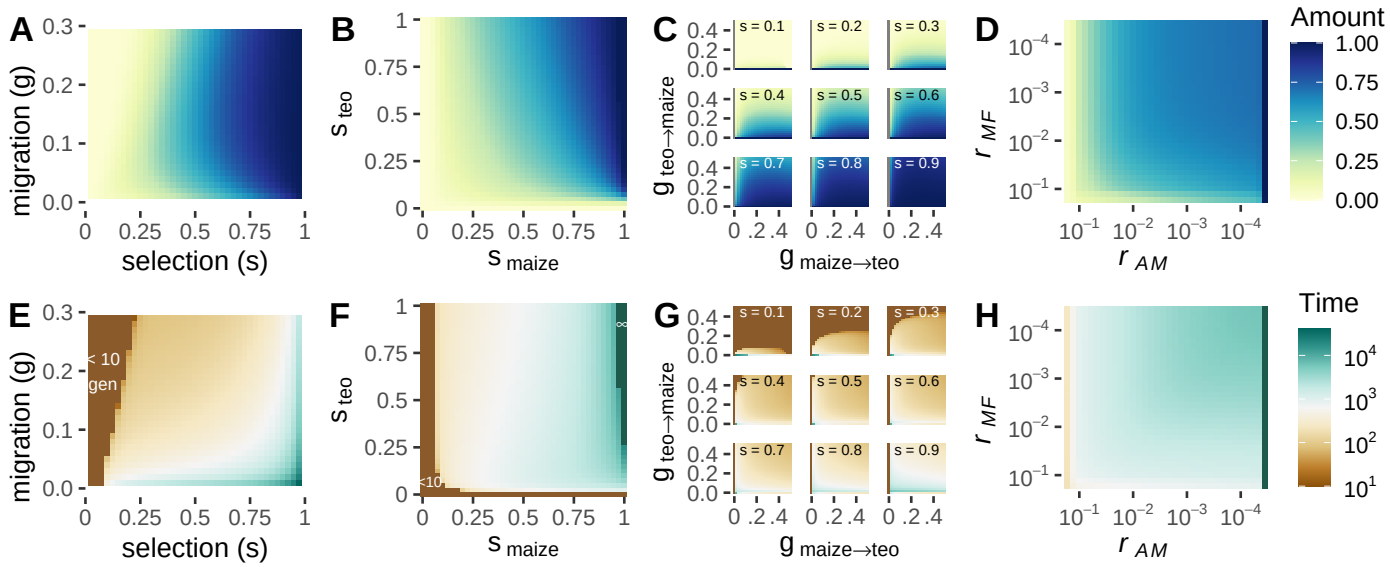

Figure 4 The maximum amount (A – D) and duration (E – H) of reinforcement: Reinforcement as a function of symmetric selection and migration (**A** and **E** with $r_{\mathcal{AM}} = r_{\mathcal{MF}} = 10^{-4}$), different selection coefficients in maize and teosinte (**B** and **F**, with $g_{\text{maize}\to\text{teo}} = g_{\text{teo}\to\text{maize}} = 0.03$ and $r_{\mathcal{AM}} = r_{\mathcal{MF}} = 10^{-4}$), asymmetric migration rates across numerous selection coefficients (**C** and **G**, with $r_{\mathcal{AM}} = r_{\mathcal{MF}} = 10^{-4}$), and recombination rates (**D** and **H**, with a symmetric selection coefficient of 0.8 and $g_{\text{maize}\to\text{teo}} = g_{\text{teo}\to\text{maize}} = 0.03$). Note that the x-axis in figures **D** and **H** moves from loose linkage on the left to tight linkage on the right. Complete or non-transient reinforcement is visible on the far right of figures **F** and **H**, indicated by the darkest green time duration, and the ∞ symbol in **F**. The amount of reinforcement is quantified as $(p_{[z,\text{gen=x}]} - p_{[z,\text{gen=0}]})/p_{[z,\text{gen=0}]}$, where p_z equals the probability of being fertilized by non-migrant pollen, scaled by the frequency of non-migrant pollen grains ("gen" refers to time in generations).

sexual conflict over reinforcement and the evolutionary traces it leaves behind—namely the adaptive spread of female barriers in one species/population and the adaptive introgression of male compatibility alleles into the other. These results provide a rich set of predictions and interpretations of empirical patterns that were absent from previous game theoretic (Parker and Partridge 1998; Gavrilets and Hayashi 2005) and verbal (Coyne and Orr 2004) models.

In our model, sexual selection favors a male gametic trait that overcomes a heterospecific female barrier. This poses a conflict: females are selected to avoid the production of maladapted hybrids, while male gametes that increase their fertilization success will generally be favored. In our model, the breakdown of reproductive isolation is marked by the rapid adaptive introgression of the male compatibility factor into maize, following recombination onto the locally adapted haplotype. Back-migration of this allele into the teosinte population hastens its fixation across populations. The final step in the model is the slow homogenization of the female barrier allele across demes, as the male compatibility allele fixes in both, rendering the isolating barrier allele ineffective. Ultimately, we show that barriers acting at different stages of hybridization can affect how reinforcement proceeds. Below we discuss the relationship of our results to previous theory, implications for the process of reinforcement, and empirical implications for hybridizing *Zea mays* subspecies and other taxa.

Theoretical context and predictions for reinforcement

Previous models of reinforcement treated the sexes interchangeably (Felsenstein 1981), or assumed assortative mating under female control (Lande 1981; Servedio and Kirkpatrick 1997; Kelly and Noor 1996), either by "matching" or classical "preference/trait" mechanisms of assortative mating (Kopp *et al.* 2018) (but see Spencer *et al.* 1986, as a notable exception). Both matching and classical preference/trait models induce a trade-off between interspecific and intraspecific mating: a male with a trait favored by heterospecific females will have limited mating success with conspecific females.

While numerous studies have addressed the role of introgression in reinforcement (e.g. Sanderson 1989; Liou and Price 1994; Kirkpatrick and Servedio 1999; Servedio 2000; Matute 2010a), a distinguishing feature of our model is the mechanism of non-random fertilization, which we model as a PMPZ incompatibility functioning like a gametophytic factor in *Zea mays* (Kermicle 2006) and PMPZ barriers in broadcast spawners (e.g. Lessios 2007). In our incompatibility-based model, introgression of a male compatibility allele is facilitated by the fact that it does not prevent intraspecific mating—that is, by definition our model lacks an evolutionary trade-off between intra- and interspecific mating. As such, (in)compatibility type mating interactions can result in the transient evolution of reinforcement, while matching or classic preference/trait models cannot.

In general, premating barriers will incur more similar opportunity costs to males and females, thus minimizing sexual conflict, while opportunity costs might differ between sexes for PMPZ isolation. However, certain physical and/or biochemical properties of PMPZ interactions may minimize the opportunity for interspecific sexual conflict by enforcing a trade-off between overcoming a heterospecific barrier and successfully fertilizing conspecifics, which would allow for the evolutionary stability of reinforcement. For example, as Howard (Howard 1993) argued, and Lorch & Servedio (Lorch and Servedio 2007) showed, a pref-

bioRxiv preprint doi: https://doi.org/10.1101/2020.11.10.377481; this version posted August 18, 2021. The copyright holder for this preprint (which was not certified by peer review) is the author/funder, who has granted bioRxiv a license to display the preprint in perpetuity. It is made available under aCC-BY-NC-ND 4.0 International license.

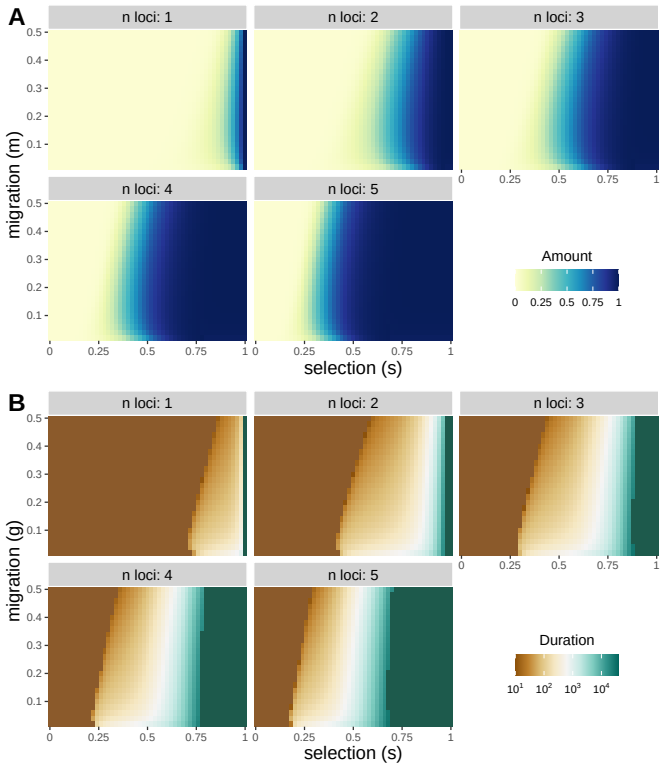

Figure 5 Oligogenic ecological selection: The maximum strength (**A**) and duration (**B**) of reinforcement with ecological selection at n loci, where all ecologically selected loci are unlinked to one another and to the gametophytic factor. The selection coefficient s against a maladaptive allele is multiplicative within and among loci – e.g. the fitness of an individual homozygous for the locally maladaptive allele at all n loci is $(1-s)^{2n}$). Migration rate g is symmetric and recombination rate $r_{\mathcal{MF}} = 10^{-4}$.

erence for conspecific sperm can stably evolve to minimize interspecific fertilization. Thus we expect conspecific sperm precedence in competitive fertilization to allow stable (non-transient) reinforcement by PMPZ isolation (e.g. Castillo and Moyle 2019). Likewise, mechanistic features of non-competitive fertilization can also induce a trade-off between inter- and intraspecific crossing success. For example, if pollen must grow an optimal distance to fertilize an ovule (as observed in interspecific *Nicotiana* crosses Lee *et al.* 2008), success on both inter- and intraspecific styles is impossible. Finally, if reinforced prezygotic barriers operate like the two-locus incompatibility in our model (e.g. if one species evolved preference for a neutral trait ignored by the other species), there would be no opportunity cost and we expect dynamics identical to those in our model.

The role of sexual conflict and sexual selection in reinforcement

Our model shows that the common phenomenon of sexual conflict (see Arnqvist and Rowe 2005, for examples), wherein male and female interests are misaligned, can erode reinforcement by PMPZ incompatibilities. This role for sexual conflict in removing species boundaries runs counter to the conventional role it is thought to play in speciation (Van Doorn *et al.* 2001; Gavrilets and Waxman 2002; Rice 1996, but see Parker and Partridge (1998)). Previous theory (Gavrilets and Waxman 2002) and experiments (Palopoli *et al.* 2015), as well as natural patterns of reproductive isolation (Brandvain and Haig 2005; Ting *et al.* 2014) and diversification rates (Arnqvist *et al.* 2000) suggest that independent coevolutionary arms races between male and female traits in two incipient species can pleiotropically result in behavioral or mechanical isolation. In this manner, intraspecific sexual conflict was thought to be an "engine of speciation" (Rice *et al.* 2005).

By contrast, we show that the interspecific conflict between the sexes over fertilization hampers speciation by undermining the evolution of reinforcement. This highlights an under-appreciated challenge to reinforcement by PMPZ barriers. Broadly, our results align with studies suggesting that incompatibilities (Bank *et al.* 2012), especially those with a transmission advantage (Meiklejohn *et al.* 2018), can adaptively introgress across species boundaries.

Servedio & Bürger (Servedio and Bürger 2014) found that Fisherian sexual selection can undermine reinforcement, and specifically that movement of female preference alleles across species can favor heterospecific male traits by sexual selection even when such traits are disfavored by natural selection. Their model incorporates a mating advantage to maladaptive male traits, which undermines the evolution of reinforcement. In contrast, our model shows that the benefit of siring low fitness hybrids (when the alternative is missed fertilization opportunities that result in no offspring) can also undermine the evolution of reinforcement. Counter to expectations of the Servedio & Bürger (Servedio and Bürger 2014) model, the stylar barrier allele in our model is at low frequency for a substantial period of time in maize, as it is disfavored while the locally adaptive trait is in linkage disequilibrium with the male compatibility allele. As such, our models make contrasting predictions: Servedio & Bürger's model (Servedio and Bürger 2014) predicts that alternative female preferences will coexist in both populations early in the evolutionary process, while our model predicts that female preference for the "wrong" species signal will only become common in both populations very late in the process of genetic exchange, once the male trait is fixed and the preference is moot.

Our model can be seen as a specific instance of the lek paradox (Borgia 1979), as a female preference ultimately erodes variation for a male trait. Following previous proposed resolutions of the lek paradox (e.g. Rowe and Houle 1996), Proulx (Proulx 2001) suggested that a female preference for an indicator of paternal fitness (e.g. sperm competitiveness) could act as a "single allele" mechanism of reinforcement (sensu Felsenstein 1981). Under a model of local adaptation, however, the efficacy of this resolution depends on details of population structure. In our model, rather than being resolved, the lek paradox leaves a signature of the "ghost of reinforcement past."

Empirical implications, predictions, and interpretation of current observations

We show that reinforcement by PMPZ incompatibilities is quite precarious. As such, to the extent that such barriers do not incur a trade-off between conspecific and heterospecific fertilization success, we predict that reinforcement by PMPZ barriers should be rare. Thus, the finding that gametic isolation in broadcast spawners is not the product of reinforcement (contrary to initial claims e.g. (Geyer and Palumbi 2003), discussed in Vacquier and Swanson 2011), as well as meta-analyses showing that PMPZ isolation does not differ between sympatric and allopatric species

bioRxiv preprint doi: https://doi.org/10.1101/2020.11.10.377481; this version posted August 18, 2021. The copyright holder for this preprint (which was not certified by peer review) is the author/funder, who has granted bioRxiv a license to display the preprint in perpetuity. It is made available under aCC-BY-NC-ND 4.0 International license.

pairs in *Drosophila* (Turissini and Matute 2017) or across three angiosperm genera (Moyle *et al.* 2004), are consistent with our model.

However, this negative evidence is not necessarily evidence for the negative. While a dearth of evidence of reinforcement by PMPZ isolation is consistent with our theory, the few documented cases in which PMPZ barriers are reinforced allow for better evaluation of its predictions. Specifically, we predict that reinforcement by PMPZ barriers involves *(1)* recent sympatry, so that the male barrier has not yet taken off, or *(2)* a trade-off between male success in overcoming inter- and intraspecific postmating barriers, as is found in preference/trait mechanisms, or *(3)* unidirectional gene flow, and/or *(4)* exceptionally strong postzygotic isolation, such that gene flow is vanishingly rare.

Poikela *et al.* (Poikela *et al.* 2019) found elevated PMPZ isolation in *D. flavomontana* populations recently sympatric with *D. montana*, suggesting reinforcement by PMPZ isolation in this case, but found evidence for reinforcement by premating isolation in populations sympatric for longer periods. Again, while reinforcement by PMPZ isolation in a recently sympatric population and reinforcement by premating isolation in a population sympatric for longer does not prove that reinforcement by PMPZ isolation was transient, it is consistent with this theoretical prediction. In another convincing case, Castillo and Moyle (Castillo and Moyle 2019) observed elevated conspecific sperm precedence for *D. pseudoobscura* in populations sympatric with *D. persimilis* (Castillo and Moyle 2019). While the reciprocal cross direction was not examined in this study, sympatric males with a competitive advantage over conspecifics were out-competed by allopatric conspecifics, suggesting an underlying trade-off in sperm performance. Kay (Kay and Schemske 2008; Yost and Kay 2009) found strong evidence consistent with reinforcement by PMPZ isolation between wild gingers *C. scaber* and sympatric *C. pulverulentus*. Intriguingly, gene flow in this case is unidirectional (Kay 2006) and is therefore consistent with predictions from out model. Reinforcement by PMPZ isolation in *D. yakuba* and *D. santomea* is most difficult to reconcile with our model, as they have a stable hybrid zone, no evidence of conspecific sperm precedence, and bidirectional hybridization (Matute 2010b). However, Turissini *et al.* (Turissini and Matute 2017) observed only short (i.e. very old) blocks of introgression in this species pair, suggesting nearly no ongoing gene flow. In sum, our theory could explain the existing cases of reinforcement by PMPZ isolation, and generates specific hypotheses to be tested in additional systems.

Study limitations and predictions for maize and teosinte

Our model is inspired by PMPZ incompatibilities in *Zea mays* subspecies. However, we simplified this system for analysis, and parameter values and modelling choices are not carefully calibrated to the biology of this or any other system. Most notably, we assumed only two populations, a single gametophytic factor, and a simple multiplicative fitness function across a small number of divergently selected loci. Our model revealed that strong ecological selection is required for PMPZ incompatibility to evolve by reinforcing selection. Yet this requirement became less stringent as we included more loci, which suggests that the genetic architecture of local adaptation is a key area for further exploration.

It is difficult to choose an appropriate model for local adaptation and linkage between locally adaptive alleles and PMPZ incompatibilities. Adaptive differentiation can be controlled by few (Selby and Willis 2018; Lowry and Willis 2010) or many (Yeaman 2013) loci; and the linkage between locally adaptive alleles and PMPZ incompatibilities is biologically variable, and rarely known. Intriguingly, *tga1* and *su1*, two "domestication" loci likely experiencing strong divergent selection in maize and teosinte, are relatively close (within 10 centiMorgans) to one gametophytic factor, suggesting that our simple single adaptive locus model may be consistent with some features of this system Wang *et al.* (2005); Whitt *et al.* (2002). However, at least three gametophytic factors—tightly linked pairs of $\mathcal{M}$ and $\mathcal{F}$ loci—exist in this subspecies pair. The other gametophytic factors in *Z. mays* are not closely linked to loci known to experience strong divergent selection, suggesting that more complex architecture must be incorporated to explain the evolution of all known gametophytic factors upon secondary contact between maize and teosinte. Simultaneously considering all gametophytic factors that isolate teosinte from maize—as the stylar barrier seems to always arise in *Z. m. mexicana*, not maize—could better predict their frequencies, which are known to differ across populations (e.g. Kermicle 2006; Kermicle *et al.* 2006; Kermicle and Evans 2010).

Our work follows a simplification of empirical patterns known from hybridizing *Z. mays* subspecies. That is, we assume that M is initially common and F rare in teosinte, and does not address the origins of gametophytic factors. While the initial divergence at the pollen allele is outside the scope of our model, it could be explained by pleiotropy: gametophytic factors in *Z. mays* are members of the multi-function pectin methylesterase (PME) and pectin methylesterase inhibitor (PMEI) gene families (Moran Lauter *et al.* 2017; Lu *et al.* 2014, 2019, 2020) and could be favored by mechanisms related to other functions. Notably, one large subclass of PMEs contain both PME and PMEI domains, providing a potential explanation for tight linkage of the M and F alleles (Tian *et al.* 2006). Alternatively, these loci may have evolved to prevent polyspermy (a known risk to embryo viability in maize (Grossniklaus 2017)), or M and F could have initially swept together by Fisherian runaway selection (as proposed by Jain Jain 1967), followed by the decay of F, which is neutral once M is fixed. As such, the origin of gametophytic factors by either runaway selection or pleiotropy could explain the tight linkage between pollen and style alleles found in maize (Lu *et al.* 2014), which does not strongly impact the evolution of reinforcement (Fig. S5).

This work was motivated by an empirical riddle. Despite both an opportunity for reinforcement (gene flow occurs between subspecies, and hybrids have reduced but non-zero fitness in either parental environment (Wilkes 1977; Hufford *et al.* 2012, although clear cases of adaptive introgression and deliberate hybridization by farmers exist)), and the observation that stylar incompatibilities are common in *Z. mays* ssp. *mexicana* sympatric with maize, "[t]he unexpected presence of the [male compatibility] allele in sympatric landrace maize appear[ed]... to negate any effect of [the] crossing barrier", puzzling researchers (Kermicle *et al.* 2006). Our model explains this observation as the initial evolution of reinforcement while the stylar barrier adaptively spreads through teosinte, followed by the adaptive introgression of teosinte pollen compatibility alleles into maize. We suggest that in most sympatric populations, at most gametophytic factors, the stylar fertilization barrier (the F allele) rapidly swept through teosinte (Phase 1 in Figure 2), and the pollen compatibility allele (M) has adaptively introgressed into sympatric highland maize landraces (Phase 2 in Figure 2). In this case,

bioRxiv preprint doi: https://doi.org/10.1101/2020.11.10.377481; this version posted August 18, 2021. The copyright holder for this preprint (which was not certified by peer review) is the author/funder, who has granted bioRxiv a license to display the preprint in perpetuity. It is made available under aCC-BY-NC-ND 4.0 International license.

our expectation from empirical observations suggests that these populations are in the slow final phase of our model, in which allele frequencies at the stylar barrier slowly equilibrate. Future work should evaluate how this model applies to other biological contexts, by incorporating a large number of adaptive loci sprinkled across a realistic genome, including the fitness effects of intrinsic genetic barriers (Dobzhansky-Muller Incompatibilities), and/or the modelling of more realistic population structures.

Materials and Methods

Quantifying reinforcement and its duration: We summarized our results by quantifying the duration and maximum extent of reinforcement. We quantified the amount of reinforcement at generation g as $(p_{[z,\text{gen=g}]} - p_{[z,\text{gen=0}]})/p_{[z,\text{gen=0}]}$. p_z equals the probability of being fertilized by non-migrant pollen, scaled by the frequency of non-migrant pollen grains. We quantified the duration of reinforcement as the number of generations for which the amount of reinforcement was greater than 0.05.

Computer Code: All code is written in R (R Core Team 2020) and is available at https://github.com/carushworth/gametotheory. We generated figures with the ggplot2 (Wickham 2016) and cowplot (Wilke 2020) packages, and used the dplyr (Wickham *et al.* 2020) package to process numeric results.

Partitioning selection: In a sense, all selection for or against the female incompatibility allele, F, is indirect, as it does not itself impact fitness. Nonetheless, we aim to partition total selection for (or against) the F allele into selection for reinforcement and linked selection. In this exercise, we ignore the change in frequency of paternally-derived genotypes (which includes migration, fertilization, and selection), as none of this change is plausibly attributable to the F allele.

We first compute the difference in allele frequency between maternally-derived haplotypes in offspring after vs. before selection as $\Delta p_{F,\text{mat}}$ directly from our results. $\Delta p_{F,\text{mat}} = p_{F,\text{mat-derived after sel}} - p_{F,\text{mom}}$. We then decompose $\Delta p_{F,\text{mat}}$ into components of reinforcing and linked selection:

$$\Delta p_{F,\text{mat}} = \Delta p_{F,\text{mat, Reinforcement}} + \Delta p_{F,\text{mat, Linked}} \quad (2)$$

Each generation we find $\Delta p_{F,\text{mat, Linked}}$ by calculating $\Delta p_{F,\text{mat}}$ under the counterfactual case of random fertilization. We then find the change in frequency of F by reinforcing selection $\Delta p_{F,\text{mat, Reinforcement}}$ by rearranging Eq. 2.

Acknowledgments

This work was funded by NSF award #1753632 to J Ross-Ibarra, MMS Evans, and Y Brandvain. We are grateful to Robin Hopkins and Maria Servedio, whose comments greatly improved the manuscript, and to Jerry Kermicle for helpful conversation. We would like to acknowledge Felix Andrews for the smorgasbord of statistical advice, although we did not follow it.

References

Arnqvist, G., M. Edvardsson, U. Friberg, and T. Nilsson, 2000 Sexual conflict promotes speciation in insects. Proceedings of the National Academy of Sciences **97**: 10460–10464.

Arnqvist, G. and L. Rowe, 2005 *Sexual conflict*. Princeton University Press.

Bank, C., R. Bürger, and J. Hermisson, 2012 The limits to parapatric speciation: Dobzhansky-Muller incompatibilities in a continent-island model. Genetics **191**: 845–63.

Barghi, N., J. Hermisson, and C. Schlötterer, 2020 Polygenic adaptation: a unifying framework to understand positive selection. Nature Reviews Genetics **21**: 1–13.

Borgia, G., 1979 Sexual selection and the evolution of mating systems. In *Sexual Selection and Reproductive Competition in Insects*, edited by M. S. Blum and N. A. Blum, pp. 19–80, Academic Press.

Brandvain, Y. and D. Haig, 2005 Divergent mating systems and parental conflict as a barrier to hybridization in flowering plants. Am Nat **166**: 330–8.

Calfee, E., D. Gates, A. Lorant, M. T. Perkins, G. Coop, *et al.*, 2021 Selective sorting of ancestral introgression in maize and teosinte along an elevational cline. bioRxiv **10.1101/2021.05.06.442525**.

Castillo, D. M. and L. C. Moyle, 2019 Conspecific sperm precedence is reinforced, but postcopulatory sexual selection weakened, in sympatric populations of *Drosophila*. Proc Biol Sci **286**: 20182535.

Coyne, J. A. and A. Orr, 2004 *Speciation*. Sinauer.

Dobzhansky, T., 1937 *Genetics and the Origin of Species*. Columbia University Press.

Felsenstein, J., 1981 Skepticism towards Santa Rosalia, or why are there so few kinds of animals? Evolution **35**: 124–138.

Gavrilets, S., 2014 Is sexual conflict an "engine of speciation"? Cold Spring Harb Perspect Biol **6**: a017723.

Gavrilets, S. and T. Hayashi, 2005 Speciation and sexual conflict. Evolutionary Ecology **19**: 167–198.

Gavrilets, S. and D. Waxman, 2002 Sympatric speciation by sexual conflict. Proc Natl Acad Sci U S A **99**: 10533–8.

Geyer, L. and S. Palumbi, 2003 Reproductive character displacement and the genetics of gamete recognition in tropical sea urchins. Evolution **57**: 1049–60.

Grossniklaus, U., 2017 Polyspermy produces tri-parental seeds in maize. Current Biology **27**: R1300–R1302.

Hopkins, R., R. Guerrero, M. Rausher, and M. Kirkpatrick, 2014 Strong Reinforcing Selection in a Texas Wildflower. Current Biology **24**: 1995 – 1999.

Howard, D. J., 1993 Reinforcement: Origin, dynamics, and fate of an evolutionary hypothesis. In *Hybrid zones and the evolutionary process*, edited by R. G. Harrison, pp. 46–69, Oxfprd University Press, Oxford.

Hufford, M. B., P. Lubinksy, T. Pyhäjärvi, M. T. Devengenzo, N. C. Ellstrand, *et al.*, 2013 The genomic signature of crop-wild introgression in maize. PLoS Genet **9**: e1003477.

Hufford, M. B., X. Xu, J. Van Heerwaarden, T. Pyhäjärvi, J.-M. Chia, *et al.*, 2012 Comparative population genomics of maize domestication and improvement. Nature Genetics **44**: 808.

Jain, S. K., 1967 Population dynamics of a gametophytic factor controlling selective fertilization. Genetica **38**: 485–503.

Kay, K. M., 2006 Reproductive isolation between two closely related hummingbird-pollinated neotropical gingers. Evolution **60**: 538–52.

Kay, K. M. and D. W. Schemske, 2008 Natural selection reinforces speciation in a radiation of neotropical rainforest plants. Evolution **62**: 2628–42.

Kelly, J. K. and M. A. Noor, 1996 Speciation by reinforcement: A model derived from studies of *Drosophila*. Genetics **143**: 1485–97.

Kermicle, J., S. Taba, and M. Evans, 2006 The gametophyte-1 locus and reproductive isolation among *Zea mays* subspecies. Maydica **51**: 219–225.

Kermicle, J. L., 2006 A selfish gene governing pollen-pistil com-

bioRxiv preprint doi: https://doi.org/10.1101/2020.11.10.377481; this version posted August 18, 2021. The copyright holder for this preprint (which was not certified by peer review) is the author/funder, who has granted bioRxiv a license to display the preprint in perpetuity. It is made available under aCC-BY-NC-ND 4.0 International license.

patibility confers reproductive isolation between maize relatives. Genetics **172**: 499–506.

Kermicle, J. L. and M. M. S. Evans, 2010 The *Zea mays* sexual compatibility gene *ga2*: Naturally occurring alleles, their distribution, and role in reproductive isolation. Journal of Heredity **101**: 737–749.

Kirkpatrick, M., 2001 Reinforcement during ecological speciation. Proc Biol Sci **268**: 1259–63.

Kirkpatrick, M. and V. Ravigné, 2002 Speciation by natural and sexual selection: Models and experiments. Am Nat **159 Suppl 3**: S22–35.

Kirkpatrick, M. and M. R. Servedio, 1999 The Reinforcement of Mating Preferences on an Island. Genetics **151**: 865–884.

Kopp, M., M. R. Servedio, T. C. Mendelson, R. J. Safran, R. L. Rodríguez, *et al.*, 2018 Mechanisms of assortative mating in speciation with gene flow: Connecting theory and empirical research. Am Nat **191**: 1–20.

Lande, R., 1981 Models of speciation by sexual selection on polygenic traits. Proceedings of the National Academy of Sciences **78**: 3721–3725.

Lee, C. B., L. E. Page, B. A. McClure, and T. P. Holtsford, 2008 Post-pollination hybridization barriers in *Nicotiana* section *Alatae*. Sexual Plant Reproduction **21**: 183.

Lessios, H., 2007 Reproductive isolation between species of sea urchins. Bulletin of Marine Science **81**: 191–208.

Liou, L. W. and T. D. Price, 1994 Speciation by reinforcement of premating isolation. Evolution **48**: 1451–1459.

Lorch, P. D. and M. R. Servedio, 2007 The evolution of conspecific gamete precedence and its effect on reinforcement. J Evol Biol **20**: 937–49.

Lowry, D. B. and J. H. Willis, 2010 A widespread chromosomal inversion polymorphism contributes to a major life-history transition, local adaptation, and reproductive isolation. PLOS Biology **8**: 1–14.

Lu, Y., S. A. Hokin, J. L. Kermicle, T. Hartwig, and M. M. S. Evans, 2019 A pistil-expressed pectin methylesterase confers cross-incompatibility between strains of *Zea mays*. Nature Communications **10**: 2304.

Lu, Y., J. L. Kermicle, and M. M. S. Evans, 2014 Genetic and cellular analysis of cross-incompatibility in *Zea mays*. Plant Reprod **27**: 19–29.

Lu, Y., A. N. Moran Lauter, S. Makkena, M. P. Scott, and M. M. S. Evans, 2020 Insights into the molecular control of cross-incompatibility in *Zea mays*. Plant Reproduction **33**: 117–128.

Matute, D. R., 2010a Reinforcement can overcome gene flow during speciation in *Drosophila*. Current Biology **20**: 2229–2233.

Matute, D. R., 2010b Reinforcement of gametic isolation in *Drosophila*. PLoS Biol **8**: e1000341.

Meiklejohn, C. D., E. L. Landeen, K. E. Gordon, T. Rzatkiewicz, S. B. Kingan, *et al.*, 2018 Gene flow mediates the role of sex chromosome meiotic drive during complex speciation. Elife **7**.

Metz, E. C., R. E. Kane, H. Yanagimachi, and S. R. Palumbi, 1994 Fertilization between closely related sea urchins is blocked by incompatibilities during sperm-egg attachment and early stages of fusion. Biol Bull **187**: 23–34.

Moran Lauter, A. N., M. G. Muszynski, R. D. Huffman, and M. P. Scott, 2017 A Pectin Methylesterase ZmPme3 Is Expressed in Gametophyte factor1-s (Ga1-s) Silks and Maps to that Locus in Maize (*Zea mays* L.). Frontiers in Plant Science **8**: 1926.

Moyle, L. C., M. S. Olson, and P. Tiffin, 2004 Patterns of reproductive isolation in three angiosperm genera. Evolution **58**: 1195–208.

Palopoli, M. F., C. Peden, C. Woo, K. Akiha, M. Ary, *et al.*, 2015 Natural and experimental evolution of sexual conflict within *Caenorhabditis nematodes*. BMC Evolutionary Biology **15**: 93.

Parker, G. A. and L. Partridge, 1998 Sexual conflict and speciation. Philos Trans R Soc Lond B Biol Sci **353**: 261–74.

Poikela, N., J. Kinnunen, M. Wurdack, H. Kauranen, T. Schmitt, *et al.*, 2019 Strength of sexual and postmating prezygotic barriers varies between sympatric populations with different histories and species abundances. Evolution **73**: 1182–1199.

Proulx, S. R., 2001 Female choice via indicator traits easily evolves in the face of recombination and migration. Evolution **55**: 2401–2411.

R Core Team, 2020 *R: A Language and Environment for Statistical Computing*. R Foundation for Statistical Computing, Vienna, Austria.

Rice, W. R., 1996 Sexually antagonistic male adaptation triggered by experimental arrest of female evolution. Nature **381**: 232–4.

Rice, W. R., J. E. Linder, U. Friberg, T. A. Lew, E. H. Morrow, *et al.*, 2005 Inter-locus antagonistic coevolution as an engine of speciation: Assessment with hemiclonal analysis. Proc Natl Acad Sci U S A **102 Suppl 1**: 6527–34.

Ross-Ibarra, J., M. Tenaillon, and B. S. Gaut, 2009 Historical divergence and gene flow in the genus *Zea*. Genetics **181**: 1399–1413.

Rowe, L. and D. Houle, 1996 The lek paradox and the capture of genetic variance by condition dependent traits. Proceedings of the Royal Society of London. Series B: Biological Sciences **263**: 1415–1421.

Sanderson, N., 1989 Can gene flow prevent reinforcement? Evolution **43**: 1223–1235.

Selby, J. P. and J. H. Willis, 2018 Major QTL controls adaptation to serpentine soils in *Mimulus guttatus*. Molecular Ecology **27**: 5073–5087.

Servedio, M. R., 2000 Reinforcement and the genetics of nonrandom mating. Evolution **54**: 21–29.

Servedio, M. R. and R. Bürger, 2014 The counterintuitive role of sexual selection in species maintenance and speciation. Proc Natl Acad Sci U S A **111**: 8113–8.

Servedio, M. R. and M. Kirkpatrick, 1997 The effects of gene flow on reinforcement. Evolution **51**: 1764–1772.

Servedio, M. R. and M. A. Noor, 2003 The role of reinforcement in speciation: Theory and data. Annual Review of Ecology, Evolution, and Systematics **34**: 339–364.

Spencer, H. G., B. H. McArdle, and D. M. Lambert, 1986 A theoretical investigation of speciation by reinforcement. The American Naturalist **128**: 241–262.

Swanson, W. J. and V. D. Vacquier, 1998 Concerted evolution in an egg receptor for a rapidly evolving abalone sperm protein. Science **281**: 710–2.

Tian, G.-W., M.-H. Chen, A. Zaltsman, and V. Citovsky, 2006 Pollen-specific pectin methylesterase involved in pollen tube growth. Developmental Biology **294**: 83–91.

Ting, J. J., G. C. Woodruff, G. Leung, N.-R. Shin, A. D. Cutter, *et al.*, 2014 Intense Sperm-Mediated Sexual Conflict Promotes Reproductive Isolation in *Caenorhabditis* Nematodes. PLOS Biology **12**: 1–14.

Turissini, D. A. and D. R. Matute, 2017 Fine scale mapping of genomic introgressions within the *Drosophila yakuba* clade. PLOS Genetics **13**: 1–40.

Turissini, D. A., J. A. McGirr, S. S. Patel, J. R. David, and D. R.

bioRxiv preprint doi: https://doi.org/10.1101/2020.11.10.377481; this version posted August 18, 2021. The copyright holder for this preprint (which was not certified by peer review) is the author/funder, who has granted bioRxiv a license to display the preprint in perpetuity. It is made available under aCC-BY-NC-ND 4.0 International license.

Matute, 2017 The rate of evolution of postmating-prezygotic reproductive isolation in *Drosophila*. Molecular Biology and Evolution **35**: 312–334.

Vacquier, V. D. and W. J. Swanson, 2011 Selection in the rapid evolution of gamete recognition proteins in marine invertebrates. Cold Spring Harbor Perspectives in Biology **3**: a002931.

Van Doorn, G. S., P. C. Luttikhuizen, and F. J. Weissing, 2001 Sexual selection at the protein level drives the extraordinary divergence of sex-related genes during sympatric speciation. Proc Biol Sci **268**: 2155–61.

Veller, C., N. B. Edelman, P. Muralidhar, and M. A. Nowak, 2019 Recombination, variance in genetic relatedness, and selection against introgressed DNA. bioRxiv **10.1101/846147**.

Wallace, J., S. Larsson, and E. Buckler, 2014 Entering the second century of maize quantitative genetics. Heredity **112**: 30–38.

Wang, H., T. Nussbaum-Wagler, B. Li, Q. Zhao, Y. Vigouroux, *et al.*, 2005 The origin of the naked grains of maize. Nature **436**: 714–719.

Wang, M., Z. Chen, H. Zhang, H. Chen, and X. Gao, 2018 Transcriptome analysis provides insight into the molecular mechanisms underlying gametophyte factor 2-mediated cross-incompatibility in maize. Int J Mol Sci **19**.

Whitt, S. R., L. M. Wilson, M. I. Tenaillon, B. S. Gaut, and E. S. Buckler, 2002 Genetic diversity and selection in the maize starch pathway. Proceedings of the National Academy of Sciences **99**: 12959–12962.

Wickham, H., 2016 *ggplot2: Elegant Graphics for Data Analysis*. Springer-Verlag New York.

Wickham, H., R. François, L. Henry, and K. Müller, 2020 *dplyr: A Grammar of Data Manipulation*. R package version 1.0.2.

Wilke, C. O., 2020 *cowplot: Streamlined Plot Theme and Plot Annotations for 'ggplot2'*. R package version 1.1.0.

Wilkes, H. G., 1977 Hybridization of maize and teosinte in mexico and guatemala and the improvement of maize. Economic Botany **31**: 254–293.

Yeaman, S., 2013 Genomic rearrangements and the evolution of clusters of locally adaptive loci. Proceedings of the National Academy of Sciences **110**: E1743–E1751.

Yost, J. M. and K. M. Kay, 2009 The evolution of postpollination reproductive isolation in *Costus*. Sex Plant Reprod **22**: 247–55.

bioRxiv preprint doi: https://doi.org/10.1101/2020.11.10.377481; this version posted August 18, 2021. The copyright holder for this preprint (which was not certified by peer review) is the author/funder, who has granted bioRxiv a license to display the preprint in perpetuity. It is made available under aCC-BY-NC-ND 4.0 International license.

Supplement

Supp. Text S1: Pseudo-code for our model

We forward iterated genotype frequencies over time, not by iterating a numerical equation, but rather by deterministic programmatic iteration of a the evolutionary process. Our R scripts are included as a supplemental file, but here we provide pseudo-code to describe the process to the reader.

1. **Initiation:** Beginning with user-specified initial allele frequencies in each population, as well as additional parameters (e.g. the number of unlinked, local adaptation loci), we build initial genotype frequencies, assuming linkage equilibrium and random mating within each population.

2. **Iteration:** Every generation, we iterate the evolutionary process, for both populations – one population at a time – by

   (a) *Meiosis in males:* Generating haploid pollen grans from diploid genotypes by meiosis, using genotype frequencies in the previous generation.

   (b) *Migration:* Making a pollen pool with haplotype frequencies $L'_{ix} = L_{ix} - m(L_{ix} - L_{iy})$. Recall that m denotes the proportion of pollen in population x which migrated from population y.

   (c) *Pollination and Fertilization:* We assume that, after migration, pollen from the pollen pool falls randomly on styles within the population, so the frequency of mating between a given pollen haplotype and stylar genotype (with frequencies from this population after the conclusion of the previous generation) is their product. Fertilization is non-random, with c indicating the strength of discrimination against incompatible m alleles. For a given diploid stylar genotype, the frequency of paternal genomes with alleles A and a are p_A and $p_a \times (1-c)$, respectively, with each divided by the proportion of pollen compatible with that stylar genotype (all pollen for ff genotypes and $(1-c) \times p_{M\text{pollen after migration}}$ for Ff and FF genotypes).

   (d) *Female meiosis and syngamy:* Finally, females undergo meiosis and zygotes are generated at random, conditional on compatibility between stylar genotypes and pollen haplotype (above).

   (e) *Selection:* We count the number of alleles at all $\mathcal{A}$ loci that mismatch the environment, n_{maladapt}, and calculate the fitness of each genotype as $(1 - n_{\text{maladapt}})^s$. We calculate mean fitness as the product of genotype fitness and genotype frequency, summed over all genotypes. Finally, we find the frequency of each genotype after selection as the product of its frequency before selection and its fitness, divided by mean fitness.

   (f) *Return summary:* We return a vector of genotype frequencies, as well as the extent of reinforcement in this population in this generation (as described in the Methods). Optional returns are available (e.g. partitioning allele frequency change across the life cycle, and evaluating "counterfactual scenarios" for selection for reinforcement and linked selection on F), which we only used for a few exemplary scenarios to minimize computational and storage expense.

   (g) *Repeat or conclude:* After conducting the steps above for both populations, we store the new genotypes' frequencies, as well as other quantities of interest. The simulation then returns to (a) if stopping criteria have not been met, or concludes if so. By default, stopping criteria are: simulation length of at least 1000 generations and genotype frequencies at equilibrium (identified when the sum of the absolute value of genotype frequency change across all phased genotypes in both populations is less than 0.00001).

3. **Conclusion:** At the conclusion of the simulation, we return phased $\mathcal{AMF}$ genotype frequencies after selection in each population for every generation, the extent of reinforcement every generation, as well as optional summaries mentioned above (see code for all options).

Supp. Text S2: Notation for gametophytic factors

Our notation throughout differs from the existing literature on gametophytic factors. In this literature, each of the three known gametophytic factors (Ga1, Ga2, and Tcb1) is represented as a single locus with three haplotypes (e.g. Moran Lauter *et al.* 2017). The "strong"' haplotype, indicated by s or S, contains both functional alleles from this study (F and M). The haplotype with only the pollen-expressed compatibility allele is referred to as m, and is equivalent to the Mf genotype in the present study. The non-functional allele is referred to in the literature in lowercase (e.g. ga1, ga2, tcb1), and is equivalent to the mf genotype in our study. The mF genotype is not known in the wild.

Supp. Text S3: Mathematical Appendix

We present standard recursion equations to provide some intuition for our results, but note that we did not use these recursions to generate our figures, which come from a iteration of the process rather than an explicit recursion of 27 unphased (64 phased) genotype frequencies in two non-randomly mating populations. Nor do we provide quasi-linkage equilibrium or Hardy-Weinberg equilibrium approximations as our focus is on the exact results provided in the main text. As such, the equations below, which largely recapitulate standard results from population genetic theory, are meant to provide some mathematical intuition for our results.

bioRxiv preprint doi: https://doi.org/10.1101/2020.11.10.377481; this version posted August 18, 2021. The copyright holder for this preprint (which was not certified by peer review) is the author/funder, who has granted bioRxiv a license to display the preprint in perpetuity. It is made available under aCC-BY-NC-ND 4.0 International license.

Migration All alleles change in frequency by migration in the same manner. Allele frequencies in pollen at the ith locus in the focal population x after migration, L'_{ix}, equal

$$L'_{ix} = L_{ix} - g_{\mathrm{y}\to\mathrm{x}}(L_{ix} - L_{iy}) \tag{3}$$

Where the prime $'$ denotes the frequency in pollen after pollen migration and L_{iy} is the allele frequency in the other population. From Eq 3, the change in allele frequency at the ith locus in pollen grains by pollen migration equals $\Delta_{L'_{ix}\text{ migration}} = -g_{\mathrm{y}\to\mathrm{x}}(L_{ix} - L_{iy})$, a standard result in population genetics.

Fertilization We assume both no pollen limitation, and an infinite supply of pollen, such that the frequency of a pollen haplotype on a stigma equals the frequency of this pollen haplotype in the local environment. Under this model, selection during fertilization changes the frequency of alleles in paternally-derived haplotypes relative to their frequency in pollen after migration, and does not impact allele frequencies of maternally-derived haplotypes.

After mating, the frequency of paternally-derived haplotypes bearing the pollen allele is $p_{M''}$, with the double prime denoting that frequencies are calculated after migration and fertilization. This value depends on the relative advantage of the pollen compatibility allele on a given stylar genotype, $\widetilde{c_i}$ (that is, the relative fitness of the compatible pollen haplotype M on a the ith stylar genotype), weighted by the frequency of the ith diploid stylar genotype at the $\mathcal{F}$ locus (i.e. before migration), p_i:

$$p_{M''} = \sum \widetilde{c_i} p_i \tag{4}$$

Where $\widetilde{c_i} = 1/(1 - c_i p_{m'})$. If the stylar barrier is dominant, $c_{FF} = c_{Ff} = c$ and $c_{ff} = 0$, and $p_{M''} = (1 - p_{ff})\frac{p_{M'}}{1-cp_{m'}} + p_{ff}p_{M'}$. We can then find $\Delta p_{\text{ fertilization}}$ as

$$\begin{aligned}
\Delta p_{\text{ fertilization}} &= p_{M''} - p_{M'} \\
&= (1 - p_{ff})(\frac{p_{M'}}{1 - cp_{m'}} - p_{M'}) + p_{ff}(p_{M'} - p_{M'}) \\
&= (1 - p_{ff})(\frac{p_{M'}}{1 - cp_{m'}} - p_{M'}) \\
&= (1 - p_{ff})(\frac{p_{M'}}{1 - cp_{m'}} - \frac{p_{M'}(1 - cp_{m'})}{1 - cp_{m'}}) \\
&= (1 - p_{ff})(\frac{cp_{M'}p_{m'}}{1 - cp_{m'}})
\end{aligned} \tag{5}$$

Equation 5 is the standard allele frequency change from population genetics weighted by the frequency with which selection can operate – i.e. the frequency of incompatible styles.

Linked selection during fertilization. We now consider the change in frequency of an allele (A or F, described below as X which includes both alleles) in linkage disequilibrium with the pollen incompatibility allele M due to the mating advantage of M.

After mating, we calculate the frequency of paternally-derived haplotypes bearing this linked allele, $p_{X''}$, where the double prime indicates that the frequency is calculated after both migration and mating. This quantity depends on the advantage of the pollen compatibility allele on a given stylar genotype and the statistical association between alleles M and X (described by gametic phase linkage disequilibrium, D_{MX}, which is the covariance between M and X alleles in pollen after pollen migration), weighted by the marginal frequency of the diploid genotype at the $\mathcal{F}$ locus in styles (i.e. before migration), p_i.

$$p_{X''} = p_{FF} \times \frac{p'_X + c(D'_{MX} + p'_x p'_m)}{1 - cp'_m} + p_{Ff} \times \frac{p'_X + c(D'_{MX} + p'_x p'_m)}{1 - cp_m} + p_{ff} \times \frac{p'_X}{1} \tag{6}$$

The change in frequency of an allele linked to $\mathcal{M}$ between pollination and fertilization is therefore

$$\Delta p_{X\text{ fertilization}} = (1 - p_{ff})\frac{c \times D'_{MX}}{1 - cp'_m} \tag{7}$$

As such, the alleles in positive linkage disequilibrium with the pollen compatibility allele M always increase in frequency during fertility selection because of the fertilization advantage, so long as there are some incompatible styles in the population. Because linkage disequilibrium between M and F, as well as M and A, is never less than zero, all teosinte alleles increase in frequency in both populations by fertility selection (Figure 3B).

The generation of *trans* linkage disequilibrium during fertilization. We begin with two diverged populations, fixed for alternative alleles at local adaptation and pollen compatibility loci and with different allele frequencies at the stylar incompatibility. As such, LD between pollen compatibility and locally adaptive alleles is initially very large, and is broken down by migration and recombination.

The pollen-style incompatibility system generates *trans* LD between pollen and stylar loci – that is, compatibility rules generate a statistical association between paternally-derived M alleles and maternally derived F alleles. Before selection, this *trans* LD equals

$$D_{MF,trans} = \frac{cp'_m p'_M p_F p_{ff}}{1 - cp'_m} \tag{8}$$

bioRxiv preprint doi: https://doi.org/10.1101/2020.11.10.377481; this version posted August 18, 2021. The copyright holder for this preprint (which was not certified by peer review) is the author/funder, who has granted bioRxiv a license to display the preprint in perpetuity. It is made available under aCC-BY-NC-ND 4.0 International license.

Clearly, this also indirectly generates *trans* LD between maternally-derived stylar incompatibilities and loci in LD with the pollen compatibility allele (or deviations from Hardy-Weinberg equilibrium at the F locus). *Trans* LD is converted to *cis* LD by recombination.

Local adaptation Genotype frequencies at the local adaptation locus $\mathcal{A}$ after selection follow the standard population genetic equation $p_i^{'} = p_i w_i / \overline{w}$.

With multiplicative fitness effects, at a single local adaptation locus in the population in which A is favored, genotypic fitnesses are: $w_{AA} = 1$, $w_{Aa} = (1-s)$, and $w_{aa} = (1-s)^2$, and mean fitness equals $\overline{w} = 1 - 2p_a s + s^2 p_{aa}$. After selection, genotype frequencies are:

$$\begin{aligned} p_{AA,\text{next gen}} &= \frac{p_{AA}^{'''}}{\overline{w}} \\ p_{Aa,\text{next gen}} &= \frac{p_{Aa}^{'''}(1-s)}{\overline{w}} \\ p_{aa,\text{next gen}} &= \frac{p_{aAa}^{'''}(1-s)^2}{\overline{w}} \end{aligned} \tag{9}$$

and the change in genotype frequencies between fertilization and viability selection are

$$\begin{aligned} \Delta p_{AA,\text{next gen}} &= \frac{p_{AA}^{'''} - \overline{w} p_{AA}^{'''}}{\overline{w}} = \frac{s p_{AA}^{'''}(2p_a^{'''} - s p_{aa}^{'''})}{\overline{w}} \\ \Delta p_{Aa,\text{next gen}} &= \frac{p_{Aa}^{'''}(1-s) - \overline{w} p_{Aa}}{\overline{w}} = -\frac{s p_{Aa}^{'''}(1 - 2p_a^{'''} + s p_{aa}^{'''})}{\overline{w}} \\ \Delta p_{aa,\text{next gen}} &= \frac{p_{aAa}^{'''}(1-s)^2 - \overline{w} p_{aa}^{'''}}{\overline{w}} = \frac{-2s p_{aa}^{'''}(1 - p_a^{'''} - s(1 - p_{aa}^{'''})/2)}{\overline{w}} \end{aligned} \tag{10}$$

.

With multiplicative fitness, the locally maladapted allele always decreases by direct selection, regardless of allele frequency or inbreeding coefficient (Fig. S7).

Linked selection during local selection. After fertilization, selection directly changes the frequency of the local adaptation loci as described above. This also changes the frequency of loci statistically associated with the locally adapted allele. The change in frequency of an allele, X (e.g. F or M), linked to $\mathcal{A}$ by linked selection is determined by the selection coefficient s and zygotic LD, and equals:

$$\begin{aligned} \Delta X = & \frac{s(2D_{XX,A} + D_{Xx,A}) + s^2(D_{XX,aa} + D_{Xx,aa}/2)}{1 - 2p_a s + s^2 p_{aa}} \\ & \text{where} \\ D_{XX,A} &= p_{XX} p_a - p_{XXa} \\ D_{Xx,A} &= p_{Xx} p_a - p_{Xxa} \\ D_{XX,aa} &= p_{XXaa} - p_{XX} p_{aa} \\ D_{Xx,aa} &= p_{Xxaa} - p_{Xx} p_{aa} \end{aligned} \tag{11}$$

bioRxiv preprint doi: https://doi.org/10.1101/2020.11.10.377481; this version posted August 18, 2021. The copyright holder for this preprint (which was not certified by peer review) is the author/funder, who has granted bioRxiv a license to display the preprint in perpetuity. It is made available under aCC-BY-NC-ND 4.0 International license.

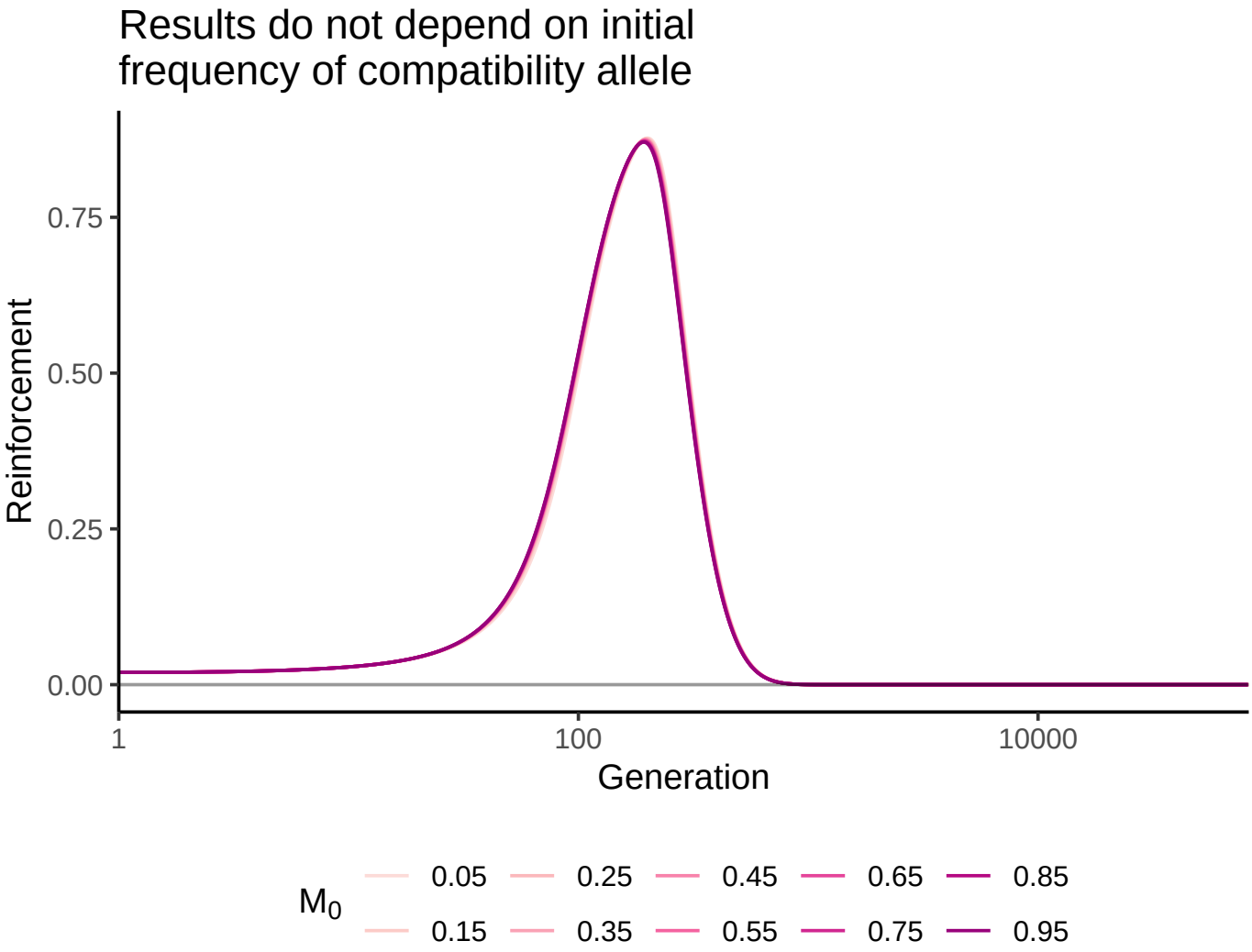

Figure S1 Results are robust to initial frequency of M in teosinte. The impact of variability in the initial frequency of pollen compatibility allele, M, in teosinte on the transient reinforcement of postmating prezygotic isolation (note all lines are on top of one another). Parameter values: Selection — $s_{\text{teo}} = s_{\text{maize}} = 0.75$. Migration — ($g_{\text{maize}\to\text{teo}} = g_{\text{teo}\to\text{maize}} = 0.1$). Recombination — $r_{\mathcal{AM}} = r_{\mathcal{MF}} = 0.0001$. Allele frequencies — $f_{M0,\text{teo}} =$ displayed by color, $f_{M0,\text{maize}} = 0$, $f_{F0,\text{teo}} = 0.01$, $f_{F0,\text{maize}} = 0$.

bioRxiv preprint doi: https://doi.org/10.1101/2020.11.10.377481; this version posted August 18, 2021. The copyright holder for this preprint (which was not certified by peer review) is the author/funder, who has granted bioRxiv a license to display the preprint in perpetuity. It is made available under aCC-BY-NC-ND 4.0 International license.

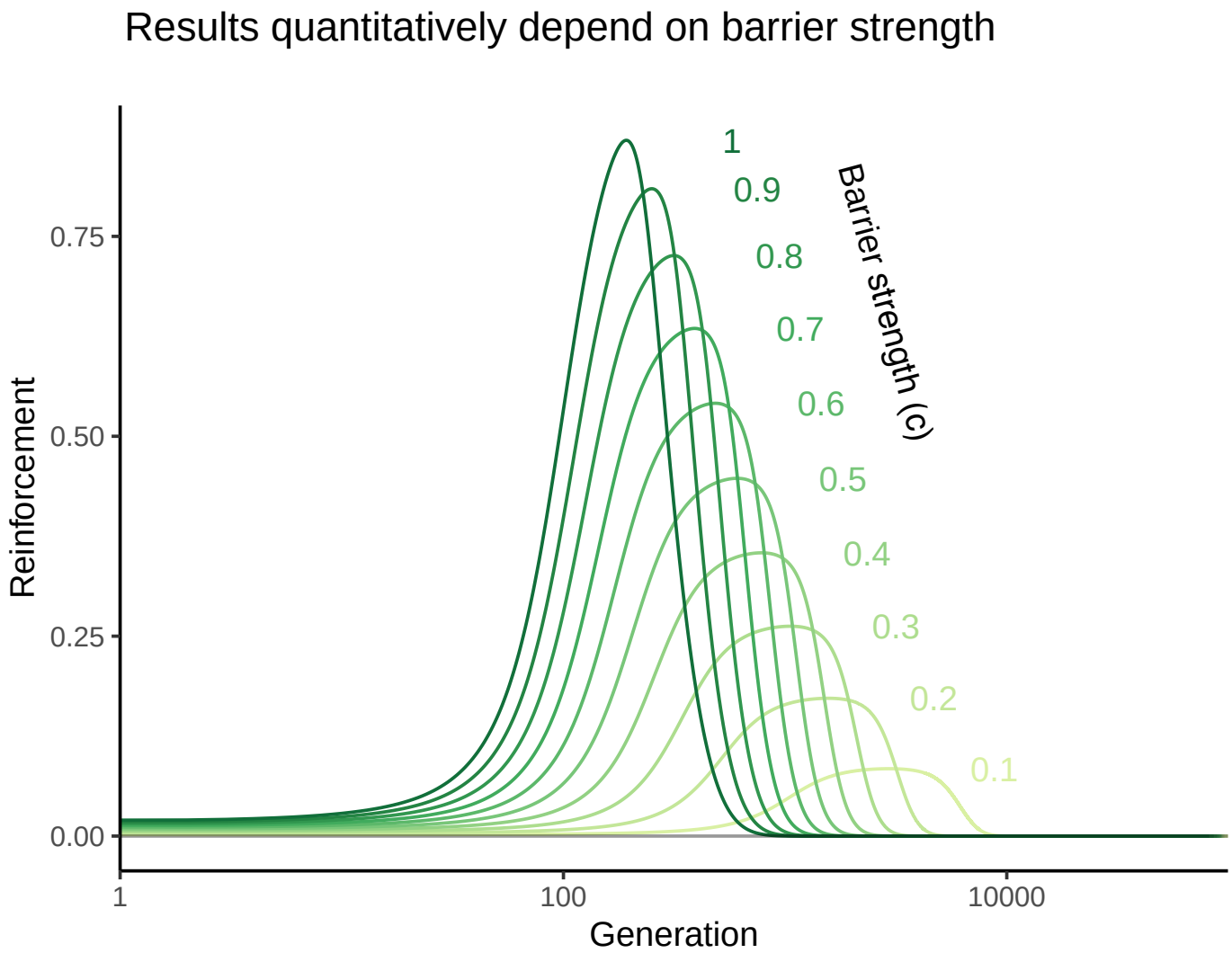

Figure S2 Results change quantitatively with incomplete barriers. We allow for an imperfect barrier by asserting that styles with fertilization barrier genotypes are fertilized by a given haplotype, k, with probability $x_k = \frac{p_k(1-\delta_k c)}{\sum x_k}$, where p_k is the frequency of haplotype k in pollen after fertilization, and δ_k equals zero for compatible pollen grains and one for incompatible pollen grains. c, the efficacy of the barrier, is colored in the plot above. Parameter values: Selection — $s_{\text{teo}} = s_{\text{maize}} = 0.75$. Migration — ($g_{\text{maize}\to\text{teo}} = g_{\text{teo}\to\text{maize}} = 0.1$). Recombination — $r_{\mathcal{AM}} = r_{\mathcal{MF}} = 0.0001$. Allele frequencies — $f_{M0,\text{teo}} = 1$, $f_{M0,\text{maize}} = 0$, $f_{F0,\text{teo}} = 0.01$, $f_{F0,\text{maize}} = 0$.

bioRxiv preprint doi: https://doi.org/10.1101/2020.11.10.377481; this version posted August 18, 2021. The copyright holder for this preprint (which was not certified by peer review) is the author/funder, who has granted bioRxiv a license to display the preprint in perpetuity. It is made available under aCC-BY-NC-ND 4.0 International license.

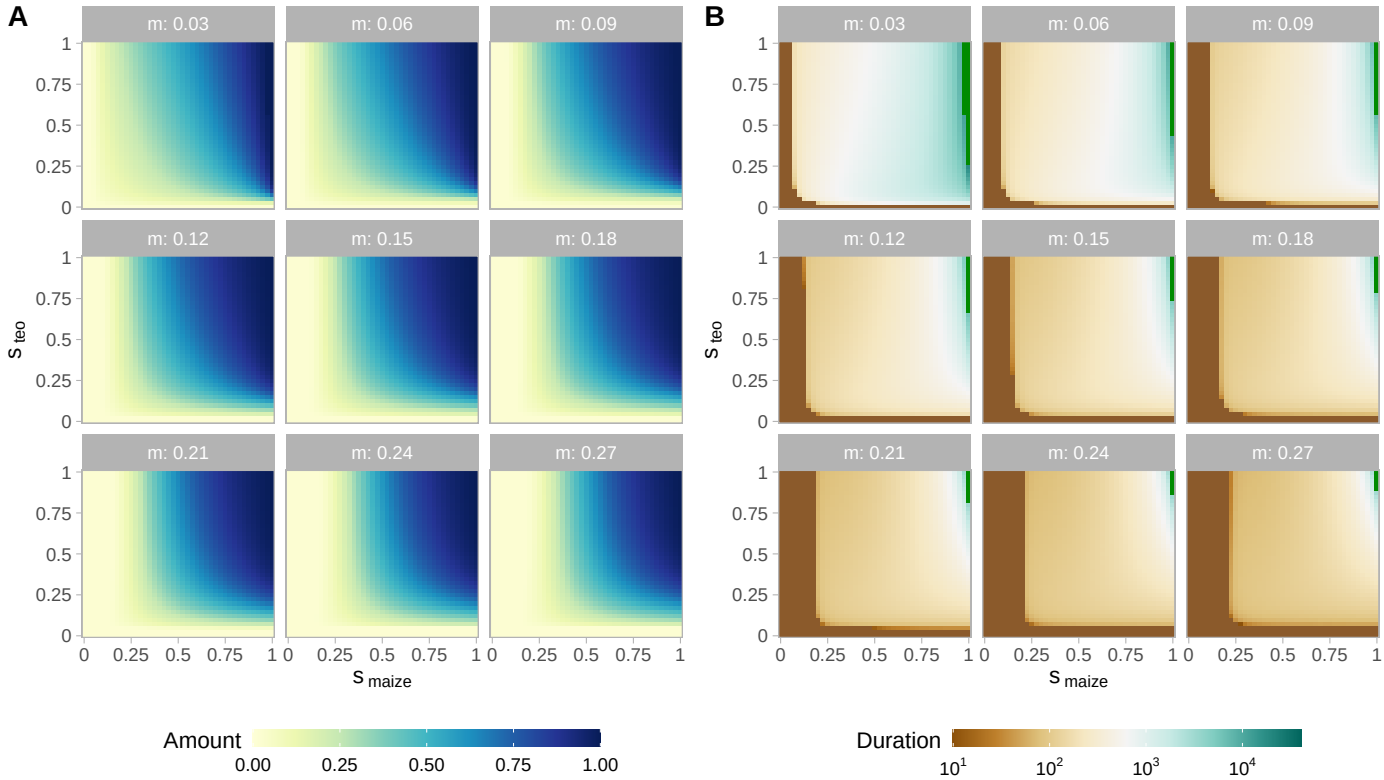

Figure S3 The impact of asymmetric selection on the extent (A) and duration (B) of reinforcement: Over a range of migration rates with $r_{\mathcal{AM}} = r_{\mathcal{MF}} = 10^{-4}$

.

bioRxiv preprint doi: https://doi.org/10.1101/2020.11.10.377481; this version posted August 18, 2021. The copyright holder for this preprint (which was not certified by peer review) is the author/funder, who has granted bioRxiv a license to display the preprint in perpetuity. It is made available under aCC-BY-NC-ND 4.0 International license.

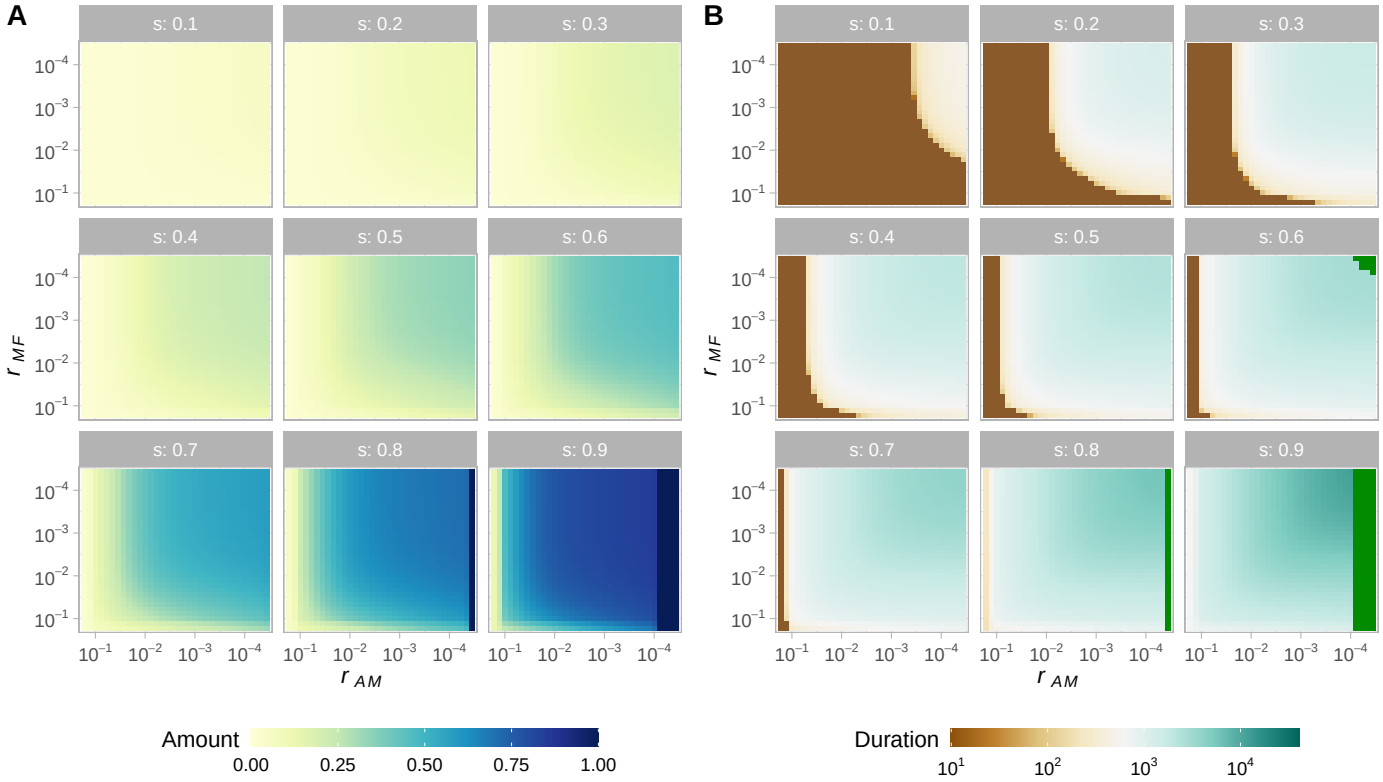

Figure S4 The impact of linkage on the extent (A) and duration (B) of reinforcement: Over a range of symmetric selection coefficients. Symmetric selection coefficient and $g_{\text{maize}\to\text{teo}} = g_{\text{teo}\to\text{maize}} = 0.03$. We note that the x-axis moves from loose linkage on the left to tight linkage on the right.

bioRxiv preprint doi: https://doi.org/10.1101/2020.11.10.377481; this version posted August 18, 2021. The copyright holder for this preprint (which was not certified by peer review) is the author/funder, who has granted bioRxiv a license to display the preprint in perpetuity. It is made available under aCC-BY-NC-ND 4.0 International license.

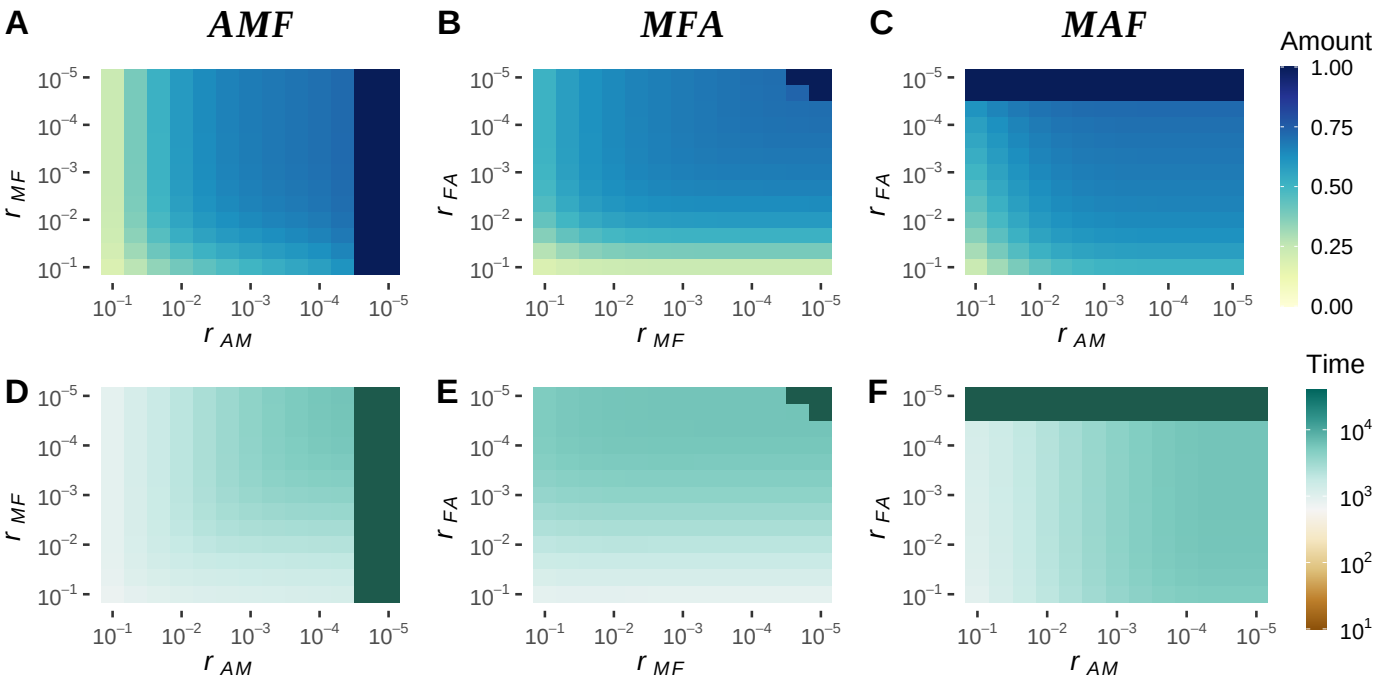

Figure S5 Locus order impacts the amount and duration of reinforcement: Reinforcement amount (**A**) and duration (**D**) with default marker order AMF; amount (**B**) and duration (**E**) under marker order MFA; amount (**C**) and duration (**F**) with marker order MAF. Shown are results with a symmetric selection coefficient of 0.8 and migration $g_{\text{maize}\to\text{teo}} = g_{\text{teo}\to\text{maize}} = 0.01$. Note that the x-axis moves from loose linkage on the left to tight linkage on the right.

bioRxiv preprint doi: https://doi.org/10.1101/2020.11.10.377481; this version posted August 18, 2021. The copyright holder for this preprint (which was not certified by peer review) is the author/funder, who has granted bioRxiv a license to display the preprint in perpetuity. It is made available under aCC-BY-NC-ND 4.0 International license.

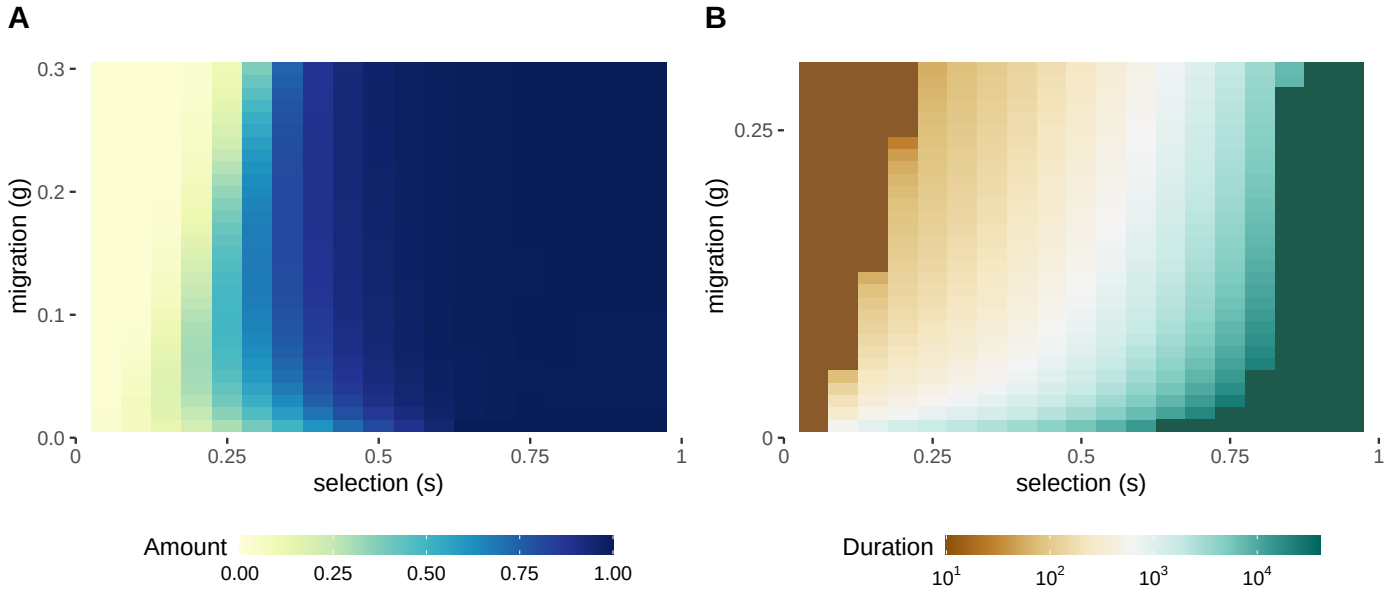

Figure S6 Asymmetrical variation in female preference does not underlie transience of reinforcement: Incorporating a second maize-acting gametophytic factor does not qualitatively change the amount (**A**) or duration of reinforcement (**B**), although reinforcement begins at lower intensities of selection and reaches completion across more selection coefficients.

bioRxiv preprint doi: https://doi.org/10.1101/2020.11.10.377481; this version posted August 18, 2021. The copyright holder for this preprint (which was not certified by peer review) is the author/funder, who has granted bioRxiv a license to display the preprint in perpetuity. It is made available under aCC-BY-NC-ND 4.0 International license.

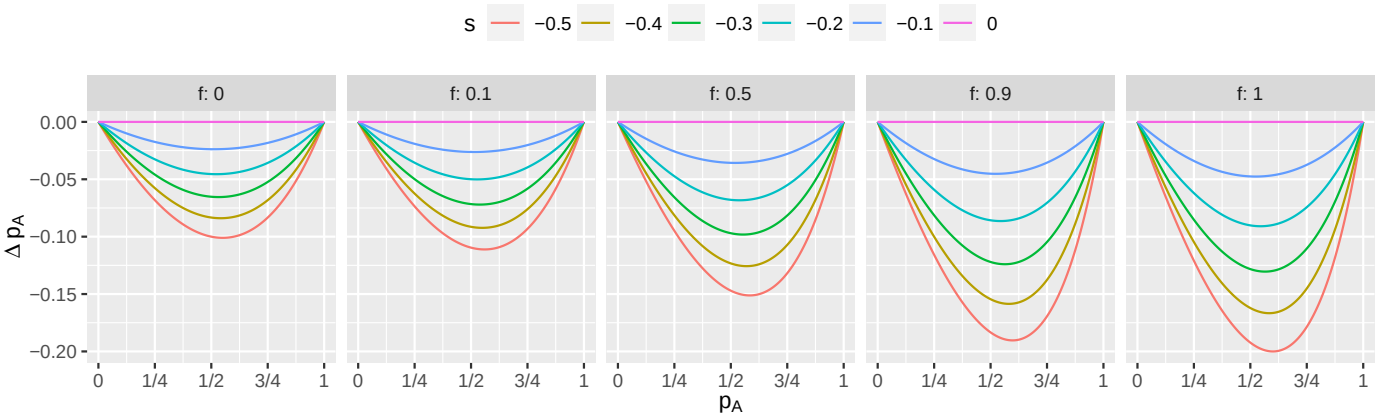

Figure S7 Allele frequency change at $\mathcal{A}$ by direct selection: The locally maladaptive allele always decreases in frequency by direct selection regardless of the degree of assortative fertilization and/ or population structure, summarized as the inbreeding coefficient, f.